Accepted Manuscript

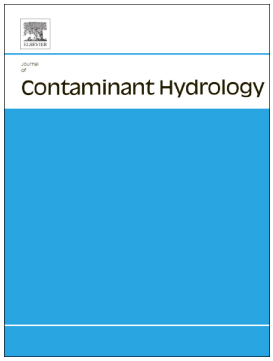

Transport of chloride and deuterated water in peat: The role of anion exclusion, diffusion, and anion adsorption in a dual porosity organic media

C.P.R. McCarter, F. Rezanezhad, B. Gharedaghloo, J.S. Price, P. Van Cappellen

PII: S0169-7722(18)30269-9
DOI: https://doi.org/10.1016/j.jconhyd.2019.103497
Article Number: 103497
Reference: CONHYD 103497

To appear in: *Journal of Contaminant Hydrology*

Received date: 4 September 2018
Revised date: 3 May 2019
Accepted date: 8 May 2019

Please cite this article as: C.P.R. McCarter, F. Rezanezhad, B. Gharedaghloo, et al., Transport of chloride and deuterated water in peat: The role of anion exclusion, diffusion, and anion adsorption in a dual porosity organic media, Journal of Contaminant Hydrology, https://doi.org/10.1016/j.jconhyd.2019.103497

This is a PDF file of an unedited manuscript that has been accepted for publication. As a service to our customers we are providing this early version of the manuscript. The manuscript will undergo copyediting, typesetting, and review of the resulting proof before it is published in its final form. Please note that during the production process errors may be discovered which could affect the content, and all legal disclaimers that apply to the journal pertain.

The final publication is available at Elsevier via https://doi.org/10.1016/j.jconhyd.2019.103497. © 2019. This manuscript version is made available under the CC-BY-NC-ND 4.0 license http://creativecommons.org/licenses/by-nc-nd/4.0/

ACCEPTED MANUSCRIPT

Transport of chloride and deuterated water in peat: The role of anion exclusion, diffusion, and anion adsorption in a dual porosity organic media

McCarter, C.P.R.[1†], Rezanezhad, F.[1], Gharedaghloo, B.[2††], Price, J.S.[2], Van Cappellen, P.[1]

[1] Ecohydrology Research Group, Department of Earth and Environmental Sciences and Water Institute, University of Waterloo, 200 University Ave West, Waterloo, ON, Canada N2L 3G1, Canada.

[2] Department of Geography and Environmental Management, University of Waterloo, 200 University Ave West, Waterloo, ON, Canada N2L 3G1, Canada.

†Currently at: Department of Physical and Environmental Sciences, University of Toronto Scarborough, 1265 Military Trail, Scarborough, M1C 1A4, Canada.

†† Currently at: Aquanty Inc., Waterloo, N2L 5C6, Canada

Corresponding author: Colin McCarter (colin.mccarter@utoronto.ca), ORCID: https://orcid.org/0000-0002-7308-0369

Key Points:

1. Chloride is not, strictly speaking, a conservative tracer
2. Chloride sorbs to peat, but the extent of binding is low and highly variable
3. Anion exclusion was observed but it did not appreciably affect chloride breakthrough
4. Chloride diffusion into immobile porosity is not governed by degree of decomposition

Keywords: Conservative Tracer; Breakthrough Curve; Equilibrium Adsorption; Pore Structure; Solute Transport

ACCEPTED MANUSCRIPT

ACCEPTED MANUSCRIPT

Abstract

The dual-porosity structure of peat and the extremely high organic matter content give rise to a complex medium that typically generates prolonged tailing and early 50% concentration breakthrough in the breakthrough curves (BTCs) of chloride (Cl^-) and other anions. Untangling whether these observations are due to rate-limited (physical) diffusion into inactive pores, (chemical) adsorption or anion exclusion remains a critical question in peat hydrogeochemistry. This study aimed to elucidate whether Cl^- is truly conservative in peat, as usually assumed, and whether the prolonged tailing and early 50% concentration breakthrough of Cl^- observed is due to diffusion, adsorption, anion exclusion or a combination of all three. The mobile-immobile (MiM) dual-porosity model was fit to BTCs of Cl^- and deuterated water measured on undisturbed cores of the same peat soils, and equilibrium Cl^- adsorption batch experiments were conducted. Adsorption of Cl^- to undecomposed and decomposed peat samples in batch experiments followed Freundlich isotherms but did not exhibit any trends with the degree of peat decomposition and sorption became negligible below aqueous Cl^- concentrations of ~310 mg L^{-1}. The dispersivity determined by fitting the Cl^- BTCs whether assuming adsorption or no adsorption were significantly different than determined by the deuterated water ($p < 0.0001$). However, no statistical differences in dispersivity ($p = 0.27$) or immobile water content ($p = 0.97$) was observed between deuterated water and Cl^- when accounting for anion exclusion. A higher degree of decomposition significantly increased anion exclusion ($p < 0.0001$) but did not influence the diffusion of either tracer into the immobile porosity. Contrary to previous assumptions, Cl^- is not truly conservative in peat due to anion exclusion, and adsorption at higher aqueous concentrations, but the overall effect of anion exclusion on transport is likely minimal.

ACCEPTED MANUSCRIPT

Introduction

Chloride (Cl^-) and other monovalent anions (e.g., bromide) have been widely used as conservative tracers in field and laboratory scale transport experiments in peat (Hoag and Price, 1997; Kleimeier et al., 2014; Kleimeier et al., 2017; McCarter et al., 2018; Ours et al., 1997; Rezanezhad et al., 2017; Rezanezhad et al., 2012) and peatlands (Baird and Gaffney, 2000; Hoag and Price, 1995; McCarter et al., 2017a; McCarter and Price, 2017). These experiments often display an early arrival of the tracer at one pore volume and a prolonged tailing, attributed to diffusion into an immobile pore region (McCarter et al., 2018). The immobile pore region is thought to consist of the hyaline cells of *Sphagnum* moss in surficial bog peat (Hoag and Price, 1997; Weber et al., 2017), or collapsed and isolated pores in more decomposed peats (Kleimeier et al., 2017). However, in other experiments, the Cl^- diffusion rate is fast enough to rapidly equilibrate with the immobile pore region, resulting in no or limited tailing but consistent early arrival of tracer at one pore volume (Hoag and Price, 1997; McCarter et al., 2018).

Hoag and Price (1995) first used sodium chloride in a field scale tracer experiment in a peatland and determined that the arrival of the tracer was delayed relative to the average linear groundwater velocity (v), yet conclusive evidence for physical retardation (by solute diffusion into the immobile porosity) could not be established as sodium (Na^+) is highly adsorptive in peat (McCarter et al., 2018; Rezanezhad et al., 2012). The field study of Hoag and Price (1995) was followed by other laboratory breakthrough curve (BTC) experiments by Hoag and Price (1997) and Ours et al. (1997) who observed Cl^- retardation in peat relative to v and attributed their findings to diffusion of Cl^- into the immobile porosity. Subsequent work at the field scale further

ACCEPTED MANUSCRIPT

illustrated the retardation of Cl^- in peatlands (McCarter and Price, 2017). The idea that prolonged tailing of Cl^- breakthrough at both field and laboratory scales is solely due to physical retardation (that is, diffusion into immobile pores) has persisted throughout the literature as the most prominent explanation of the observed data in peat (Kleimeier et al., 2017; McCarter and Price, 2017; McCarter et al., 2018; Rezanezhad et al., 2017; Rezanezhad et al., 2012; Rezanezhad et al., 2016; Simhayov et al., 2018).

The validity of the conservative nature of Cl^-, and other anions, in peat has recently been questioned (Caron et al., 2015; Liu et al., 2017). Using tritiated water and bromide, Liu et al. (2017) found no difference between the two tracers and attributed the observed prolonged tailing in their experiment to physical retardation processes, chiefly diffusion into inactive porosity or flow through a dual permeability medium. However, Liu et al. (2017) also noted that given the experimental setup the prolonged tailing could also be due to adsorption of bromide to amine groups or complexation to humic acids (Boudreau et al., 2009; Caron et al., 2015), or to hydrogen exchange with organic matter in the case of tritiated water (Sauer et al., 2009; Schimmelmann, 1991), but no evidence for these processes was provided. In poor fen peat comprising *Sphagnum* and sedge remains, McCarter et al. (2018) observed Cl^- adsorption in equilibrium batch experiments, with the data following a sigmodal (Sips) isotherm. The form of this adsorption isotherm implied that there was essentially no adsorption at low aqueous Cl^- concentrations (<500 mg L^{-1}). Yet, at higher concentrations adsorption affected the aqueous concentration, that can result in a prolonged tailing of the measured BTC (McCarter et al., 2018; Šimůnek and van Genuchten, 2008).

ACCEPTED MANUSCRIPT

In peat, the early breakthrough of anion tracers at one pore volume has been attributed to the presence of a physical immobile porosity. However, anion exclusion, which has been identified in delignified *Sphagnum russowii* cells (Richter and Dainty, 1989), could also decrease the total mobile porosity available to anions, which may partly explain the observed early breakthrough in peat. Anion exclusion has been well documented in mineral soil and is typically associated with the small micro-pores in clay sediments or a function of water films and small pores in sands and other sediments (Bresler, 1973; Gvirtzman and Gorelick, 1991; James and Rubin, 1986; Rose et al., 2009; Smith et al., 2004; Van Loon et al., 2007). Anion exclusion occurs when negatively-charged soils with small pore throats prevent the movement of anions into the hydrologically-connected pore network, typically identified by the early breakthrough of an anion tracer (Bresler, 1973; Gvirtzman and Gorelick, 1991; James and Rubin, 1986; Rose et al., 2009). Like clay soils, which have a large cation exchange capacity due their negative charge (Appelo and Postma, 2005), peat and other organic soils are predominately negatively charged (Andreasson et al., 1988; Delicato, 1996; Gogo et al., 2010; Rippy and Nelson, 2007) and can have an abundance of small pores, especially under increasing decomposition levels (Gharedaghloo et al., 2018; McCarter and Price, 2014; Rezanezhad et al., 2010). These conditions may induce anion exclusion in peat, which would decrease the time required for Cl^- detection in the effluent, similar to the presence of the immobile pore spaces. Although Richter and Dainty (1989) observed anion exclusion in delignified *Sphagnum russowii* cells, there remains no direct observation of anion exclusion affecting solute transport in peat.

Given the limited, and at times contradictory, information on Cl^- transport in peat, the primary objectives of this research were to elucidate whether the degree of decomposition affects Cl^-

ACCEPTED MANUSCRIPT

transport process and if Cl^- adsorption or anion exclusion significantly alters the determination of hydrophysical parameters derived from BTCs. To achieve these objectives, our experiments were designed to test the following two hypotheses: 1) the higher the degree of peat decomposition, the higher the Cl^- adsorption because of the increase in specific surface area, and 2) adsorption of Cl^- or anion exclusion will induce differences in the BTCs of Cl^- and deuterated water through peat. Deuterium (deuterated water, HDO) is the best conservative tracer of water movement in soils (Koeniger et al., 2010); hence, deuterated water BTCs are used here as the baseline against which the Cl^- BTCs were compared.

ACCEPTED MANUSCRIPT

ACCEPTED MANUSCRIPT

Methods

Bog peat was sampled from a hollow (i.e. between hummocks) in the Luther Marsh Wetland Conservation Area, Ontario, Canada (43°54'21" N, 80°24'21" W). The bog hollow soil profile exhibited a sharp change in peat properties from undecomposed *Sphagnum* moss, chiefly *S. rubellum* and *S. fuscum* at the surface, to relatively decomposed *Sphagnum* peat at depth, and contained relatively few woody roots. The organic matter weight fraction was between 0.88 and 0.96, and the organic carbon content varied between 0.43 to 0.47 (Gharedaghloo, 2018). Gharedaghloo and Price (2017) and Gharedaghloo and Price (2018) determined that the same peat was hydrophilic and water-wet under saturated conditions. A first peat monolith (70 × 50 × 40 cm, 0 to 40 cm below ground surface, bgs) was extracted in winter using a chainsaw to penetrate the frozen unsaturated zone and a hand-saw to detach the peat monolith from the bottom. The monolith was then placed in a plastic bin and transported to the laboratory at the University of Waterloo. To extract deeper peat (~50 to 80 cm bgs), a 20 L plastic bucket (30 cm diameter and 50 cm height) with the bottom removed was used to cut a second peat monolith out of the space cleared below the first (upper) monolith. The resulting monolith was placed in another 20 L plastic bucket for transport to the laboratory. Both upper and lower peat monoliths were placed in a -20 ˚C freezer until sub-sampling for experimentation. Although the freezing and thawing of peat can result in secondary consolidation processes, these processes are reversible (Kennedy and Price, 2005). Moreover, this peat has experienced numerous cycles of freeze and that during its development, so the implications of freezing the is likely negligible.

Equilibrium Adsorption Batch Experiments

ACCEPTED MANUSCRIPT

The peat samples were sorted in three distinct groups based on the degree of decomposition following the von Post scale of decomposition (von Post, 1926) and identified as: H1-H2 (5 – 15 cm bgs, H3-H4 (15 – 30 cm bgs), and H7 (> 50 cm bgs), herein referred to as H1, H4, and H7, respectively. One peat sample (~ 10 × 10 × 10 cm) of each group were taken from the monoliths and air dried. Milled horticultural peat (Premier Horticultural Peat), which has been used as a hydrological control in previous studies (McCarter et al., 2017b), was sieved to 1 mm and used as a control group; resulting in a total of four distinct peat types (H1, H4, H7, and Milled). For each of the peat groups, two separate batches of triplicates were used in the sorption experiments. An individual experiment consisted of 1 g of air-dried peat placed in a 60 mL glass bottle with 40 mL of the chloride-containing solution and sealed with a Teflon cap. The solutions were prepared with sodium chloride (NaCl), with Cl^- concentrations of 0.017, 0.031, 0.10, 0.31, 0.95, and 1.64 mg mL^{-1} (17, 31, 100, 305, 950, and 1640 mg L^{-1}) at pH 7. Once the bottles were filled, the samples were placed on a rotating wheel and continuously agitated for 48 h, which is an adequate time period to reach equilibrium as shown previously (Boudreau et al., 2009; Rezanezhad et al., 2012). After 48 h, the bottles were uncapped, and the resulting solutions filtered through 0.2 µm poresize polysulfone filters (ThermoFisher Scientific) into 10 mL vials for Cl^- concentration analysis by Ion Chromatography (Dionex ICS-5000; ± 3.0% error and ± 1.6% precision).

The calculated solid (*S*, adsorbed) and measured aqueous phase (*C*) Cl^- concentrations were fitted to Freundlich isotherms (Equation 1) using a least-squares regression script in MATLAB (Shimizu, 2014):

ACCEPTED MANUSCRIPT

$$S = K_F C^N \qquad \textbf{Equation 1}$$

where, S is the solid phase Cl^- concentration (mg g^{-1}), C is the aqueous phase Cl^- concentration (mg cm^{-3}), K_F is the Freundlich coefficient (mg^{1-N} g^{-1} mL^N), and N is the Freundlich exponent (-).

Breakthrough Curve Experiments

The frozen peat monoliths were sub-sampled to obtain six 10 cm long peat cores from the undecomposed (10 – 20 cm bgs) and decomposed layers (60 – 70 cm bgs). The cores were then fitted inside 10 cm high acrylic flow-through reactors (FTR) as described by Pallud et al. (2007). The key difference with the reactors used by Pallud et al. (2007) was the greater length (10 cm). The increased length to diameter (4.2 cm) ratio, relative to the original design of Pallud et al. (2007), produces a more uniform one-dimensional flow regime (Lewis and Sjöstrom, 2010) and is well above the representative elementary volume of peat (see Gharedaghloo et al. (2018) for further details). The BTCs were measured directly on the undisturbed peat cores.

After sampling, the peat cores were carefully shaved to fit the inside diameter of the FTR. The undecomposed layer comprised H1 to H4 peat, while the decomposed layer entirely comprised H7 peat. Prior to insertion into the acrylic reactors, the shaved cores were wrapped in Parafilm© and heated using a heat-gun to shrink-wrap the cores to prevent bypassing wall flow. At least 5 cm of Parafilm© was left at the top and bottom of the cores to wrap around the acrylic tube to further prevent any bypassing flow along the FTR wall. No adsorption of Cl^- to the Parafilm©

ACCEPTED MANUSCRIPT

was observed during a 72-h equilibrium batch experiment. The samples were then saturated from the bottom for 24 h in Milli-Q water to minimize entrapped air before the endcaps of the FTR were placed on the acrylic tube. A polypropylene membrane filter (0.2 µm pore size, 50 mm diameter, Pall Life Sciences) and a fibreglass filter (1 µm pore size, 47 mm diameter, Pall Life Sciences) were placed between the endcaps and sample on each end to equalize flow (see Pallud et al., 2007 for details).

The FTRs were connected to a peristaltic pump (Minipuls 3; Gilson) with equal lengths of Tygon® tubing and each FTR was individually connected to a 3-way valve. Each valve was connected to two water sources, one Milli-Q water to flush the cores and the other a tracer solution of 0.12 mg mL^{-1} Cl^- (NaCl) and +220 δ^2H (Sigma 99.9 % D_2O) as HDO. The δ^2H enrichment was far above the ~ -70 δ^2H of the Milli-Q water. The tracer solution was stored in 10 L Tedlar Bags to prevent evaporative enrichment over the course of the experiment. The cores were first flushed (3 mL h^{-1}) with Milli-Q water for 10 days to purge gas bubbles that may block flow (Lewis and Sjöstrom, 2010). After flushing, the residual Cl^- concentration in the pore water was $4.3x10^{-4}$ mg $mL^{-1)}$ (0.43 mg L^{-1}). Once purged, inflow was instantaneously switched to the tracer solution, maintaining a constant flow rate (3 mL h^{-1}, 5.2 cm day^{-1}) to begin the BTC experiment. The inflow was switched back to Milli-Q water after 5 days to capture the flushing of the tracers from the cores. Three mL of effluent of the FTRs were sampled every 5 – 6 h and immediately filtered through a 0.2 µm pore size polysulfone filter.

The filtrated outflow samples were each split into two vials, the first (1.7 mL) was analysed for deuterated water using off-axis integrated-cavity output spectroscopy (Los Gatos Research

ACCEPTED MANUSCRIPT

Liquid Water Isotope Analyser – 45 – EP; ± 0.8‰, 0.03% error) and the second (1.3 mL) was analysed for Cl^- and other common anions concentrations by Ion Chromatography (Dionex ICS-5000; ± 3.0% error and ± 1.6% precision). A zero dead-volume blank (Rajendran et al., 2008) was run with just Cl^-, as the FTR are inert to Cl^- (Pallud et al., 2007). The experiments were carried out at room temperature (22 ± 2 °C). Once the BTC experiment was completed, the bulk density (ρ) of the peat was determined by drying samples at 80°C for 48 h. Assuming a particle density (ρ_p) of 1.4 g cm^{-3} (Redding and Devito, 2006), the porosity (ϕ, Table 1) was calculated by:

$$\phi = 1 - \frac{\rho}{\rho_p} \qquad \textbf{Equation 2}$$

Breakthrough Curve Analyses

The transport of Cl^- and deuterated water were simulated using the mobile-immobile (MiM) dual-porosity model in HYDRUS-1D (Šimůnek et al., 2003; Šimůnek et al., 2008) based on the following continuity equations:

$$\frac{\delta \theta_{mo}\, c_{mo}}{\delta t} + f_{mo}\,\rho \frac{\delta s_{mo}}{\delta t} = \frac{\delta}{\delta z}\left(\theta_{mo}\, D_{mo}\, \frac{\delta c_{mo}}{\delta z}\right) - \frac{\delta q_{mo}\, c_{mo}}{\delta z} - \Gamma_s \qquad \textbf{Equation 3a}$$

and

$$\frac{\delta \theta_{im}\, c_{im}}{\delta t} + (1 - f_{mo})\rho \frac{\delta s_{im}}{\delta t} = \Gamma_s \qquad \textbf{Equation 3b}$$

with:

$$\Gamma_s = \alpha_{mim}(c_{mo} - c_{im}) + \Gamma_w^{c*} \qquad \textbf{Equation 3c}$$

ACCEPTED MANUSCRIPT

where the subscripts *mo* and *im* refer to the mobile and immobile liquid regions, respectively, θ_{mo} and θ_{im} are the volumetric moisture contents in the mobile and immobile regions ($cm^3\ cm^{-3}$) respectively, c_{mo} and c_{im} are the solute concentrations in the mobile and immobile regions (mg cm^{-3}), respectively, s_{mo} and s_{im} are the adsorbed concentrations in the mobile and immobile regions (mg g^{-1}), respectively, ρ is the bulk density (g cm^{-3}), f_{mo} is the fraction of instantaneous adsorption sites in the mobile region, q_{mo} is the volumetric fluid flux density in the mobile region (cm day^{-1}), α_{mim} is the mass transfer coefficient (day^{-1}), Γ_s is the mass transfer term for solute between the mobile and immobile regions (mg cm^{-3} day^{-1}), and Γ_w^{c*} is the transfer rate for water between the mobile and immobile region (day^{-1}). The free water diffusion coefficients (D^*) at 20°C for HDO and Cl^- were 2.3 cm^2 day^{-1} and 1.8 cm^2 day^{-1}, respectively (Appelo and Postma, 2005; Easteal et al., 1984; Murday and Cotts, 1970). The dispersion coefficient in the mobile region (D_{mo}, cm^2 day^{-1}) was determined as

$$D_{mo} = \lambda v_{mo} \qquad \textbf{Equation 4a}$$

$$v_{mo} = \frac{q_{mo}}{\theta_{mo}} \qquad \textbf{Equation 4b}$$

where, v_{mo} (cm day^{-1}) is the average linear groundwater velocity in the mobile region. The dimensionless mass transfer coefficient (ω) was determined as

$\omega = \frac{\alpha_{mim} L}{\theta_{mo} v_{mo}}$	**Equation 5**

where, L is the column length.

ACCEPTED MANUSCRIPT

The liquid flux was simulated using the van Genuchten-Mualem soil water retention and conductivity equation (Mualem, 1976; Šimůnek et al., 2008; van Genuchten, 1980) to parameterize Richard's equation (Šimůnek et al., 2008), where the total pressure gradient was equal to one and the saturated hydraulic conductivity equal to q_{mo} (5.2 cm day^{-1}) for each BTC. Under these saturated conditions, parameters of the van Genuchten-Mualem water retention curve-fitting equation (residual water content, alpha, n and l) do not affect the flow dynamics under saturated conditions and were set as constants. The residual water content (0.01), alpha (0.42 cm^{-1}), n (1.31) and l (-4.84) determined by McCarter and Price (2014) were used. Total porosity ($\phi = \theta_{mo} + \theta_{im}$) and ρ of each soil core were used as known model parameters for each FTR peat core (Table 1). Only the hydrophysical parameters (dispersivity [λ], θ_{im}, α_{mim}) were fit using deuterated water tracer. To investigate the conservative nature of Cl$^-$ as a tracer in peat, three different fitting assumptions were tested: Cl$^-$ without adsorption, Cl$^-$ with adsorption, and Cl$^-$ with anion exclusion. In HYDRUS-1D, anion exclusion can be simulated by linear partitioning coefficients (Kd) < 0, resulting in retardation coefficients (R) < 1 (Bradford et al., 2003; Rose et al., 2009; Šimůnek et al., 2003; Šimůnek et al., 2008; Šimůnek and van Genuchten, 2008). Note, when using the Kd to represent anion exclusion the effective v_{mo} increases as the Kd is < 0; whereas, under adsorption the Kd decreases the effective v_{mo} (Bradford et al., 2003; Rose et al., 2009; Šimůnek et al., 2003; Šimůnek et al., 2008; Šimůnek and van Genuchten, 2008). The retardation coefficient was determined by,

$$R = 1 + \frac{\rho Kd}{\theta} \qquad \textbf{Equation 6a}$$

$$R = \frac{v_{mo}(\theta_{mo} - \phi_{ex})}{q_{mo}} \qquad \textbf{Equation 6b}$$

ACCEPTED MANUSCRIPT

where, ϕ_{ex} is the excluded porosity due to anion exclusion. Since anion exclusion decreases the mobile porosity, the effective velocity (v_{eff}) can be determined by,

$$v_{eff} = \frac{q_{mo}}{(\theta_{eff})} \quad \textbf{Equation 7a}$$

$$\theta_{eff} = \theta_{mo} - \phi_{ex} \quad \textbf{Equation 7b}$$

where, θ_{eff} is the effective porosity. To determine the unknown parameters of the MiM model (λ, θ_{im}, α_{mim}, f_{mo}, the Freundlich adsorption model coefficients in HYDRUS-1D ($K_{F\,mim}$, N_{mim}, and *Kd*), a global search algorithm was programmed in R Statistical Software, generating 1000 realizations where the lowest 2% (n = 20) of root mean square errors (RMSE) of each global fit distribution were averaged (± 95% confidence interval, C.I.) and taken as the representative parameters of each core and tracer. The unknown parameters were randomized between defined upper and lower bounds assuming a uniform distribution for each parameter (Table S1). The effective porosity (n_e) was estimated using the drainable porosity at -100 mb measured in a Soil Moisture Equipment Corp. model 1600 pressure cell (McCarter and Price, 2017). The resulting random values of all parameters were written in the HYDRUS-1D input file to individually simulate the Cl^- (both with and without adsorption, and anion exclusion) and deuterated water BTCs. To better assess the conservative nature of chloride, as well as gain a better understanding of the diffusion processes, the Cl^- data was additionally fit by fixing the λ and θ_{im} with determined from HDO (λ_{2H} and $\theta_{im\,2H}$, respectively) and assuming anion exclusion; herein referred to as Cl^-_{HDO}. Thus, only α_{mim} and *Kd* were fit in this modelling scenario. All BTCs were normalized to the specific tracer's input concentration for display.

ACCEPTED MANUSCRIPT

The transport of solutes in peat is governed by the advective and diffusional processes in the θ_{mo}, while diffusion governs the transfer of water into/out of the θ_{im}. However, understanding the relative importance of each process is critical to correctly assessing solute transport. The Peclet number (*Pe*) illustrates the relative importance of advection or diffusion in the θ_{mo}. Following Huysmans and Dassargues (2005), *Pe* was calculated by,

$$Pe = \frac{q_{mo} L}{\theta_{mo} D^*} \qquad \textbf{Equation 8}$$

. When $Pe > 10$ diffusion is negligible to the transport of a given solute in the mobile phase (Huysmans and Dassargues, 2005). By using the D^*, rather than the effective diffusion coefficient, which is unknown, the provided *Pe*'s are a more conservative estimate. However, *Pe* only considers the flow in the θ_{mo} and not the relative importance of the mass transfer into the θ_{im}. The Damköhler number (*Da*) gives the relative importance of the diffusion rate into the θ_{im}, where,

$$Da = \frac{\alpha_{mim} L}{\nu \theta_{mo}} \qquad \textbf{Equation 9}$$

As α_{mim} increases, the *Da* will approach infinity and it is unnecessary to account for diffusion into the θ_{im} as it is assumed to be instantaneous and the convection-dispersion equation can be used for parameter estimation (Vanderborght et al., 1997; Wehrer and Totsche, 2005).

Statistical Analyses

ACCEPTED MANUSCRIPT

The RMSE between a simulated average breakthrough curve and the observed breakthrough curve data of each solute (deuterated water or Cl^-), was computed as,

$$RMSE = \left(\frac{\sum_{i=1}^{n}(Obs_i - Sim_i)^2}{n}\right)^{1/2} \quad \textbf{Equation 10}$$

where, Obs_i is the i^{th} observed point, Sim_i is the corresponding simulated concentration, and n is the number of measured points. Additionally, the Akaike Information Criterion (AIC) was calculated for all BTCs to further compare tracers and modelling scenarios,

$$AIC = 2k - 2\ln(\hat{L}) \quad \textbf{Equation 11}$$

where, k is the number of estimated parameters and $\hat{L}$ is the maximum value of the likelihood function (Akaike, 1974).

To further determine whether there were significant differences between the hydrophysical parameters (λ, θ_{im}, θ_{mo}/θ_{eff}, D_{mo}, and ν_{mo}/ν_{eff}) determined using deuterated water, Cl^- with and without adsorption, Cl^- with anion exclusion, a mixed effect model for each parameter was generated in R Statistical Software (R Development Core Team, 2018) using the distributions determined from the global searches using the *lmer* function in the *lme4* package (Bates et al., 2015; Pinheiro et al., 2018). When assuming anion exclusion, the θ_{eff} and ν_{eff} were used in place of θ_{mo} and ν_{mo}. The mixed effect model for each parameter was compared individually to the different parameter fitting assumptions (i.e., deuterated water, Cl^- with adsorption, and Cl^- without adsorption), with the sample ID nested within the sample depth (i.e., the decomposition level). The least-squares means were estimated with the *lmer* function in the *lme4* package

ACCEPTED MANUSCRIPT

(Bates et al., 2015) and statistical significance of each interaction was determined using a contrasting pair-wise comparison with Tukey adjustment using the *lsmean* function in the *lsmean* package (Lenth, 2016).

To determine the effect the degree of decomposition had on the diffusion rate into the immobile pore space and anion exclusion, the observed Cl^- data were fit to the MiM model using λ_{2H} and $\theta_{im\ 2H}$; thus, only α_{mim} and Kd were fit (Cl^-_{HDO}). To assess the relative differences between the two tracers and the undecomposed and decomposed peat, a general linear model was developed using the distributions determined from the global searches, where α_{mim} was dependent on both decomposition level and tracer (HDO or Cl^-_{HDO}) with an intercept equal to zero. A second general linear model was constructed to assess the influence of peat decomposition level on anion exclusion (R) and ϕ_{ex}, where R and ϕ_{ex} were dependent on decomposition level of the Cl^-_{HDO} results. The statistical significance of each interaction was determined using a contrasting pair-wise comparison with Tukey adjustment in the *lsmean* function in the *lsmean* package (Lenth, 2016). All statistical analyses were performed in R Statistical Software version 3.4.4 (R Development Core Team, 2018).

ACCEPTED MANUSCRIPT

Results

Adsorption Batch Experiments

Concentration dependent Cl^- adsorption was apparent at concentrations greater than 305 mg L^{-1} (0.31 mg mL^{-1}), where the local slope of the isotherm was > 0. Below this threshold adsorption was negligible and the local slope of the isotherm approached 0 (Figure 1). The K_F values ranged between 0.33 and 61.3 mg^{1-N} g^{-1} mL^N; no consistent trend between K_F and the degree of decomposition was observed. Similarly, the N parameter did not systematically vary with degree of decomposition and was typically observed to be near or above 1, except for sample H7-1 (Table 2). Only the H4 and milled peat yielded similar, near-linear isotherms for the two-individual sample batches over the concentration range tested. However, for replicates within a given batch (e.g., Batch 1 of H1 peat), the observed averages were close (Figure 1) and the resultant RMSE were acceptable (Table 2). Given the magnitude of the reported RMSE (0.19 – 15.50 mg g^{-1}; Table 2), the 17 mg L^{-1} (0.017 mg mL^{-1}) results in all samples were not reliable (i.e., the confidence intervals, C.I., were of the same magnitude as the measured values) and hence excluded from the analysis and not presented. No release of other anions (fluoride, nitrite/nitrate, sulphate, bromide, or phosphate) was observed.

Breakthrough Curve Experiments

The modelled deuterated water BTCs were in good agreement with the measured values, resulting in low RMSE (0.021 – 0.050; Table 3), with little data scatter (Figure 2). This resulted in small C.I.s for λ_{2H} and $\theta_{im\,2H}$ for all peat cores. There was a general increase in $\theta_{im\,2H}$ and λ_{2H}

ACCEPTED MANUSCRIPT

with a higher degree of decomposition, while no apparent trend in $\alpha_{mim\,2H}$ was observed (Table 3). Similar trends were observed for the parameters obtained with Cl^- BTCs (Table 4, Table S2 & Table S3). Regardless of tracer or model choice the fitted θ_{im} agreed extremely well with the measured drainable porosity at -100 mb and only when accounting for the ϕ_{ex} was a notable difference in θ_{eff} observed (Figure 3). Overall, the effluent concentrations of Cl^- exhibited more scatter than those of deuterated water (Figure 2), resulting in higher RMSE and AIC. Nevertheless, the Cl^- model fits were still in good agreement with the data, regardless of Cl^- model choice (Table 4, Table S2, and Table S3). Slightly lower RMSE were observed when not including adsorption, but all Cl^- BTC models performed worse than that of deuterated water. Typically, the AIC was lowest when assuming anion exclusion but the difference between all Cl^- models were ≤ 10 (Table 4, Table S2, and Table S3). For the Cl^- models, the lowest RMSEs were observed when assuming anion exclusion (Table 4, Table S2, and Table S3). The fitted Freundlich parameters determined from the Cl^- model with adsorption were similar across all BTCs, displaying strong non-linearity (i.e., $N_{mim} > 10$), as well as large C.I.s (Table S3). The Freundlich isotherm coefficients ($K_{F\,mim}$) varied between 1.3 and 3.2 $mg^{1-N}\,g^{-1}\,mL^{N}$ (Table S3). Although these values were within the large range determined in the adsorption batch experiments (0.33 – 61.25 $mg^{1-N}\,g^{-1}\,mL^{N}$, Table 2), the corresponding N_{mim} values (Table S3) were generally much greater than those determined in the equilibrium batch experiments (Table 2). However, both the RMSE and AIC of the adsorption models were typically greater than other two Cl^- models.

Although the BTCs were very similar between Cl^- and deuterated water, there were differences in the physical (*e.g.*, λ, θ_{im}, θ_{mo}) and flow (*e.g.*, D_{mo}) dependent parameters depending on the model

ACCEPTED MANUSCRIPT

(deuterated water, Cl^- with and without adsorption, and anion exclusion) used to derive the parameters (Figure 4). When simulated with and without adsorption, the estimated dispersivity values, λ, and D_{mo} were statistically different ($p < 0.0001$) between deuterated water and Cl^-; however, the θ_{im} and θ_{mo} values were not statistically different (Table 5). The average estimated λ using Cl^- was 2.3x and 2.4x larger than that estimated with deuterated water, without and with adsorption, respectively. However, when accounting for anion exclusion processes (Cl^-_{AE}) the estimated λ, D_{mo}, θ_{im}, and v_{eff} were not significantly different from those determined by deuterated water but the θ_{eff} was significantly lower (Table 5). However, the estimated θ_{mo} (note, $\theta_{mo} = \theta_{eff} + \phi_{ex}$) assuming anion exclusion agreed well with deuterated water and the measured drainable porosity (not shown). The random effects accounted for 41, 38, 29, 24, and 36% of the model variation for λ, D_{mo}, θ_{im}, θ_{mo}, and v_{mo} respectively. The resultant least-square means can be found in Supplementary Information (Table S4).

Anion Exclusion and Diffusion of HDO and Cl^-

Given the similarity of estimated hydrophysical parameters when accounting for anion exclusion, the Cl^- data were fit using λ_{2H} and $\theta_{im\,2H}$ to limit variability between models and assess the validity of anion exclusion assumptions. This dual tracer technique allows for the better estimation of the effect of the degree of decomposition on diffusion into the inactive porosity and anion exclusion (Cl^-_{HDO}) effects. Without assuming anion exclusion, the modelled Cl^- simulation was unable to fit the observed data under the same hydrophysical conditions (Figure 5 and Table S5). Anion exclusion significantly increased with the degree of decomposition ($p < 0.0001$), where the least-square mean R values were 0.95 and 0.87 for undecomposed and decomposed

ACCEPTED MANUSCRIPT

peat, respectively. Additionally, the ϕ_{ex} significantly increased with degree of decomposition ($p < 0.0001$). The Pe for deuterated water was well above 10 (Table 3), indicating that advective flow was dominant and that diffusion in the θ_{mo} was insignificant. Contrary to diffusion in the θ_{mo}, diffusion into the θ_{im} was an important process to consider, as the Da_{Cl-HDO} were between 1.5 – 30.4 and 0.9 – 32.2 for deuterated water and Cl^-_{HDO}, respectively. The fitted Cl^-_{HDO} resulted in similar or slightly lower RMSEs relative to the Cl^-_{AE} and Cl^-, while typically much lower AIC due to the lower number of fitted parameters (Table 6). The diffusion of both deuterated water and Cl^- were significantly different depending on the degree of decomposition but were not different between deuterated water and Cl^- within a degree of decomposition (Table 7). The differences in α_{mim} values resulted in a ratio between $\alpha_{mim\ 2H}$ and $\alpha_{mim\ Cl\ HDO}$ of 0.74 and 0.84 for undecomposed and decomposed peat, respectively (Table 8). These ratios were similar to the ratio between the free water diffusion coefficients of deuterated water and Cl^- (0.78) and fell within the 95 % C.I. for both degrees of decomposition. However, the limited sample numbers preclude further statistical analysis. The resultant least-square means can be found in Supplementary Information (Table S6).

ACCEPTED MANUSCRIPT

Discussion

Chloride Adsorption Isotherms

The Freundlich isotherm parameters vary significantly among the various batches of Luther Marsh bog peat. While isotherms for replicate samples of an individual batch were comparable, large differences were observed between batches from the same peat layer, in particular for the H1 and H7 peat (Figure 1). Furthermore, some peat samples exhibit near-linear isotherms ($N \approx 1$), while others do not (Table 2). McCarter et al. (2018) report non-linear Cl^- isotherms for undegraded poor fen peat. However, these authors found a distinct upper limit to Cl^- adsorption, which was best described by a Sips isotherm (Limousin et al., 2007; Sips, 1948). In contrast, over the concentration range tested here, no upper limit is observed for bog peat, regardless of the degree of decomposition.

One potential explanation for the highly variable isotherms is a highly heterogenous distribution of surface area in peat (Rezanezhad et al., 2016), which hinders the preparation of reproducible samples even within a single peat layer (Limousin et al., 2007). The large observed variation in isotherms suggests that a greater number of samples and mass of peat may be required to comment on the ubiquity of Cl^- adsorption in peat. Nonetheless, our results overall do not support an increase in Cl^- adsorption with increased degree of peat decomposition, as reported for cations and organic contaminants (Gharedaghloo, 2018). Possibly, this reflects the different mechanisms governing anion adsorption, compared to cations (Ho and McKay, 1999; Ho et al., 2002; McCarter et al., 2018; Rezanezhad et al., 2012) and organic molecules (Cohen et al., 1991;

ACCEPTED MANUSCRIPT

Gharedaghloo, 2018; Rutherford et al., 1992) whose adsorption chiefly depends on the specific surface area and the chemical properties of the organic matter (Andreasson et al., 1988). Further note that the Cl^- isotherms were measured at neutral pH, which is higher than found in pore waters of most bog peatlands (Glaser et al., 1997; Hayward and Clymo, 1982). At neutral pH the overall surface charge is thought to be highly negative (Andreasson et al., 1988; Delicato, 1996), suggesting that having electrostatically bound anions at low pore water ionic strengths is unlikely (Andreasson et al., 1988). However, given that the point of zero charge has been observed to be pH < 4, and perhaps pH < 2.5 for undecomposed *Sphagnum* peat (Delicato, 1996), in the low pH environments of bogs (pH ~ 4) the net surface charge would likely remain negative and similar adsorption processes where a threshold Cl^- concentration is required before Cl^- adsorption can occur. Our results clearly highlight the need for more research into the binding mechanisms of Cl^- and other anions to peat, the effect of pH on anion adsorption, and the variability of adsorption across different peat types (i.e., *Sphagnum*, sedge, or wood dominated) and degree of decomposition. Nonetheless, taken together, the observed adsorption isotherms imply that, strictly speaking, Cl^- is not an inert solute in peat, as is usually assumed. Our results, however, also indicate that Cl^- adsorption is very limited at aqueous concentrations below 0.31 mg mL^{-1} (Figure 1). Thus, at sufficiently low concentrations Cl^- should still behave as a conservative transport tracer with regards to anion adsorption. This hypothesis is further explored below.

BTC Parameter Estimation: Chloride versus Deuterated Water

Flow-through experiments are a powerful approach to characterize key reactive transport properties of porous media. Chief among these properties is the dispersivity, λ, whose accurate

ACCEPTED MANUSCRIPT

determination is crucial to reduce uncertainties in other parameter values (Šimůnek et al., 2003; Šimůnek and van Genuchten, 2008). Relative to Cl^-, deuterated water had lower parameter C.I.s, RMSE and AIC (Table 3), due to lower data scatter (Figure 2), suggesting it may be a more reliable tracer when further reactive transport modelling is required. However, the deuterated water and Cl^- when assuming anion exclusion, yield statistically indistinguishable λ, θ_{im}, and D_{mo} values and slightly lower θ_{eff}, confirming the consistency of the inferred physical flow properties of the peat and the validity of using either tracer. When assuming Cl^- adsorption to the peat, fitting all of the parameters (f_{mo}, $K_{F\,mim}$, and N_{mim}) derived from the Cl^- BTCs resulted in larger C.I.s (Table S3), suggestive of poorer parameter identifiability. The inferior performance of the Cl^- model with adsorption (i.e., higher RMSE and AIC) indicates that at the inflow concentration used (0.12 mg mL^{-1}) the adsorption of Cl^- was not a dominant process affecting Cl^- transport. This result was consistent with the equilibrium adsorption isotherms experiments, which in most cases show minimal Cl^- adsorption at aqueous concentrations below 0.31 mg mL^{-1} (Figure 1). Without the ϕ_{ex}, the θ_{mo} agreed very well with the measured drainable porosity at -100 mb (Figure 3), confirming the validity of using this measured value to fix θ_{im} as suggested by McCarter and Price (2017). Additionally, the small decrease in θ_{mo} due to the ϕ_{ex} (Table 7) did not significantly affect the flow-dependent parameters (v_{mo} and D_{mo}) (Table 5) and still fell within 0.1 of the measured drainable porosity at -100 mb (*ne*). When not accounting for anion exclusion, the estimated λ and D_{mo} were significantly different than those determined using deuterated water (Table 5). The results of the Cl^- BTC modelling indicate that anion exclusion is influencing the transport of Cl^- in peat and should potentially be accounted for if treating Cl^- as a conservative tracer. The slightly better fits of simulated concentrations assuming anion exclusion, with the observed data, and the statistically indistinguishable λ and D_{mo} parameters to

ACCEPTED MANUSCRIPT

those determined by the deuterated water BTCs, further illustrate that Cl^- is not truly conservative in peat. For example, when not assuming anion exclusion the Cl^- BTC could not be fit to the data when using the λ and θ_{im} determined using deuterated water (Table S5), while when assuming anion exclusion the observed data were successfully fit using the same parameters (Figure 5, Table 6). Therefore, in the remaining discussion we will only consider Cl^- assuming anion exclusion using the deuterated water λ and θ_{im} parameters (Cl^-_{HDO}, Table 6) and the deuterated water (Table 3) BTC modelling results.

The Role of Decomposition on Diffusion and Anion Exclusion in Peat

Using two tracers, a more representative estimation of Cl^- diffusion and anion exclusion can be achieved, where the deuterated water was used to estimate the λ and θ_{im} and Cl^- to determine $\alpha_{mim\ Cl\ HDO}$ and $Kd_{Cl\ HDO}$ (Table 6). In both cases, *Da* for both HDO and Cl^-_{HDO} between 1.5 – 30.4 and 0.9 – 32.2, respectively, suggest that diffusion into the inactive porosity remains an important process to characterize within this particular peat at the tested flow rates. Conversely, the *Pe* were all well above 10 indicating that in the θ_{mo}/θ_{eff} advection was the primary process governing the transport of all solutes and diffusion did not significantly contribute to the flux. The mass transfer coefficient of Cl^-, $\alpha_{mim\ Cl\ HDO}$, were typically slightly lower than that of deuterated water, $\alpha_{mim\ 2H}$, which was expected as the free water diffusion coefficient for Cl^- is lower than that for deuterated water (Appelo and Postma, 2005; Easteal et al., 1984; Murday and Cotts, 1970). However, the relative difference between $\alpha_{mim\ Cl^-HDO}$ and $\alpha_{mim\ 2H}$ were not distinguishable between undecomposed and decomposed samples (Table 8). The average ratios between α_{mim} values in the undecomposed peat was 0.74, lower than the ratio of the free water diffusion

ACCEPTED MANUSCRIPT

coefficients of deuterated water and Cl^- of 0.78. In contrast, the average ratio between α_{mim} values in the decomposed peat was 0.84 (Table 8). These diffusion ratio's C.I.s overlapped and encompasses the free water diffusion coefficient, suggesting that under these flow conditions changes in the peat pore structure with increasing degree of decomposition did not limit the diffusion rate between the mobile and immobile porosity and that the free water diffusion coefficient of both solutes was the governing transport property.

Recently, Simhayov et al. (2018) illustrated that in degraded and re-packed fen peat, the MiM model was not appropriate because this particular peat visually appeared, and behaved, as a single porosity media (both hydraulically and chemically) and the convection-dispersion equation could be used. In peats with a distinct dual porosity structure, the MiM model is only relevant when ω is < 100 and when this condition is violated the MiM model essentially simplifies to the convection-dispersion equation (Simhayov et al., 2018; Šimůnek et al., 2003; Šimůnek et al., 2008; Šimůnek and van Genuchten, 2008). There was large variability in the observed ω parameter for both deuterated water and Cl^-_{HDO}, where in three cases ω was near or above 100 (Table 3 and Table 6), suggesting that in these cases the data may be overparameterized and a simpler solute transport model (i.e., the convection dispersion model) would suffice. However, given the wide range of ω, and α_{mim}, parameters, there was no discernable trend to inform when to use a simplified model or the MiM. Given this, the MiM model was used for all samples to ensure consistency within the study. In any case, when ω > 100, the system is still a dual porosity media but the equilibrium time between the mobile and immobile porosities is rapid enough to treat the entire system as a single porosity medium (i.e., no observable tailing in the BTCs). Thus, there are hydrophysical conditions when the MiM

ACCEPTED MANUSCRIPT

model may be inappropriate due to overparameterization, but it may be appropriate to use the MiM model to accurately represent the physical system unless all samples within a given study allow for the use of simpler transport model.

Past studies (Gharedaghloo, 2018; Hoag and Price, 1997; Kleimeier et al., 2017; Liu et al., 2017; Liu et al., 2016; McCarter et al., 2018; Rezanezhad et al., 2017; Rezanezhad et al., 2016; Simhayov et al., 2018) have attributed the early observed breakthrough of chloride to the presence of an immobile porosity structure in the peat. While the dual porosity structure in peat is not in question, by using two "conservative" tracers, it is apparent that the early arrival of Cl^- cannot be solely accounted for due to the current dual porosity structure concept. Chloride induced pore dilation may increase the saturated hydraulic conductivity (Hoag and Price, 1997; Kettridge and Binley, 2010; McCarter et al., 2018; Ours et al., 1997) by increasing the θ_{mo} (Comas and Slater, 2004). However, the changes induced by Cl^- interactions with organic functional groups (Comas and Slater, 2004; Ours et al., 1997) would change the media properties and thus influence both tracers equally. Given the differential response in tracers and the negative charge associated with peat at pH above 4.0 (Andreasson et al., 1988; Delicato, 1996), there is clear evidence of anion exclusion at both degrees of decomposition, whereby incorporating anion exclusion processes resulted in the same hydrophysical parameter estimation as deuterated water (Table 5). Unlike single porosity soils, where anion exclusion can be identified by a decrease in λ and θ_{mo}, and subsequent increase in D_{mo} (Gvirtzman and Gorelick, 1991; James and Rubin, 1986; Van Loon et al., 2007), the λ_{Cl} increased relative to λ_{2H} in the MiM model since θ_{mo} is already represented. However, a similar result (increase in D_{mo}) can be achieved in the MiM model by increasing λ and keeping θ_{mo} constant (see equation 3a & 3b),

ACCEPTED MANUSCRIPT

which was typically observed in this study (Table S2). Similar to the traditional method of describing anion exclusion, significantly lower θ_{eff} ($p < 0.0002$) was observed when accounting for anion exclusion where $R < 1$ (Figure 3, Table 5). Without both tracers it is impossible to determine if anion exclusion is occurring, especially in a known dual porosity media. Furthermore, including the flushing curve in the BTC experiments, which many past studies have not included (Hoag and Price, 1997; Kleimeier et al., 2017; McCarter et al., 2018; Rezanezhad et al., 2017; Rezanezhad et al., 2012), highlighted the inability of Cl^- without anion exclusion to accurately describe the hydrophysical transport parameters (Table S5 and Figure 5). Only through the combination of the dual-tracer approach and investigating the injection and flushing curves was anion exclusion identified in peat.

If anion exclusion is a ubiquitous process in peat, previous estimations of the MiM parameters may overestimate the λ, as the λ_{Cl} (Table S2) was on average 2.4x larger than that of λ_{2H} (Table 3) when fitting θ_{im}, which is common in peat transport studies (Gharedaghloo, 2018; Kleimeier et al., 2017; McCarter et al., 2018; Rezanezhad et al., 2017; Rezanezhad et al., 2012; Rezanezhad et al., 2016). In these cases, as well as when fitting v_{mo} (McCarter et al., 2018; Simhayov et al., 2018) or R (Hoag and Price, 1997), the overall retardation (as determined by R) is still greater than 1 because the magnitude of anion exclusion is less than the retardation caused by the diffusion into the inactive porosity. However, when the parameter estimations are completed with fitting R in the convection dispersion equation (Hoag and Price, 1997), rather than the MiM, a more representative parameter estimation of R may be derived, as R is the total summation non-advective forces acting on the solute. In any case, given the indistinguishable parameter estimation (Table 5) between deuterated water (Table 3) and Cl^- when assuming anion exclusion

ACCEPTED MANUSCRIPT

(Table 4 and Table 6), it is possible to correctly estimate the physical parameters of peat using Cl^-, provided that anion exclusion is accounted for.

Unlike α_{mim}, where there was no difference with degree of decomposition (Table 8), the effect of anion exclusion increased ($p < 0.0001$) with degree of decomposition, as R was further from unity and ϕ_{ex} was larger with an increased degree of decomposition (Table 6). This increase in anion exclusion with increased degree of decomposition was likely due to the increasing number of smaller pores (Carey et al., 2007; Gharedaghloo, 2018; Gharedaghloo et al., 2018; McCarter and Price, 2014; Quinton et al., 2009), where the more abundant small pore throats increased the specific surface area (Gharedaghloo et al., 2018) and the overall increase in negative surface charge with increasing fulvic acid concentration (a common feature of increased degree of decomposition) led to a decrease in θ_{eff} and increased the effective pore water velocity (Bratskaya et al., 2008; Comas and Slater, 2004; Gondar et al., 2005a; Gondar et al., 2005b; Ours et al., 1997; Rose et al., 2009). These results suggest that Cl^-, and potentially other anions, may undergo anion exclusion, resulting in slightly higher effective solute velocities than predicted by a conservative tracer. Furthermore, the observed effect may be enhanced when the peat pore structure and/or experimental conditions results in the rapid equilibrium between the θ_{eff} and θ_{im} and limited to no extended tailing is observed (such as this study). However, for Cl^- the overall effect of anion exclusion remained relatively minor and the ~2x increase in λ only resulted in a maximum 0.16 decrease in R from unity. Given the dearth of knowledge regarding peat surface charge, further studies are required to better understand the exact mechanisms governing the transport of anions in peat. Moreover, as development in peatland dominated watersheds increases, the potential for unintentional contaminant release will increase. Thus, it might be

ACCEPTED MANUSCRIPT

prudent to account for anion exclusion processes, depending on the contaminant. In any case, this study represents the first identification of anion exclusion as a transport process in peat and further studies are required to establish the ubiquity of this process.

Implications of Tracer Choice on Solute Transport

The lower estimated parameter C.I.s imply that deuterated water BTCs yield parameter values with lower overall error. The decreased scatter in the observed deuterated water relative to Cl^- may in part reflect the lower analytical error in isotopic (0.3%) than chemical (3.0%) measurements; however, the relatively large difference in input concentrations may exaggerate this effect. When the larger analytical error of Cl^- is coupled with the apparent non-conservative nature of Cl^- in peat, whether due to adsorption at higher concentrations or anion exclusion, it is recommended to use enriched water isotopes as tracers rather than chemical tracers to avoid these issues. However, the relative analytical cost and time need to be weighed against the decreased total error for a given experiment, especially considering that it is generally prudent to have a greater number of replicates with lower precision than fewer replicates with higher precision (Graniero, 1999). In this study, the variability of hydrophysical parameters within a given degree of peat decomposition exceeds the C.I.s, signifying that the spatial variability can be large even among cores sampled within 50 cm of each other. In the case of anion exclusion, the overall effect is relatively minor as R approaches 1 in many cases and the deviation from 1 did not exceed 0.16. In all undecomposed cores, the R values were > 0.93 and would have a lesser influence on solute transport than the more decomposed peat with lower R values. Similarly, McCarter et al. (2018) observed that Cl^- adsorption did not significantly affect the

ACCEPTED MANUSCRIPT

transport parameters when $R = 1.07$, which is a similar absolute distance away from 1 as the anion exclusion results. It is likely that when majority of solute transport occurs in large connected pores, such as are common in poorly decomposed peat, suitable results can be obtained without including anion exclusion in the fitting routines, particularly when only the hydrophysical parameters (λ, θ_{im}, θ_{mo}, D_{mo}, and α_{mim}) are considered. However, if the goal of the study is to characterize the reactive transport of other solutes where the relative effect size may be small or concentrations low, such as trace metals, it might be prudent to use enriched water isotope tracers to characterize the flow domain rather than anion tracers to avoid potential complications with anion exclusion or adsorption. Given the logistical challenges in field-scale tracer studies (Baird and Gaffney, 2000; Balliston et al., 2018; Hoag and Price, 1995; McCarter et al., 2017a; McCarter and Price, 2017), the importance of appropriate transport model choice (Liu et al., 2017; Simhayov et al., 2018), and sample variability, Cl^- in many instances remains a suitable tracer choice.

ACCEPTED MANUSCRIPT

ACCEPTED MANUSCRIPT

Conclusions

The dual tracer approach used in this study highlighted that Cl^- is not, strictly speaking, a conservative, non-reactive tracer in peat. However, for the peat soils used here, the effect of adsorption was negligible on the BTCs obtained with an inflow concentration of 0.12 mg mL^{-1}. Anion exclusion processes resulted in significantly different hydrophysical parameter estimation than deuterated water, when this process was not accounted for in the fitting routines. Thus, for sufficiently low Cl^- concentrations, the transport of Cl^- is indistinguishable from those of deuterated water when anion exclusion processes are considered. Yet, the overall magnitude of the effect of anion exclusion in peat is minor, resulting in a maximum deviation of R from unity of 0.16. To our knowledge this is the first instance that anion exclusion has been identified in transport processes in peat, but the ubiquity of this process needs to be confirmed on a greater variety of peat types and degrees of decomposition, and the specific surface charge of the peat surface needs to be explored. This study confirmed that the saturated porosity at -100 mb is equivalent to the θ_{im} and can be fixed in the fitting routines. The observed variability within the small sample set used in this study illustrates the need for a greater number of samples and studies on these processes to better characterise transport processes in peat. Both the BTC and batch adsorption experiments imply a high spatial variability of the hydrophysical and adsorptive properties of peat, even within layers of a given degree of decomposition.

Acknowledgements

All data used are listed in the references, tables, and figures. The authors acknowledge funding through the Canada Excellence Research Chair (CERC) program to PVC. We greatly appreciate

ACCEPTED MANUSCRIPT

the excellent reviews provided by two anonymous reviewers; whose comments significantly improved the manuscript. We would also like to thank Marianne Vandergriendt, Riley Mills, and Brooke McNeil for their help in the laboratory.

ACCEPTED MANUSCRIPT

ACCEPTED MANUSCRIPT

References

Akaike, H., 1974. A new look at the statistical model identification. IEEE Transactions on Automatic Control, 19(6): 716-723.https://doi.org/10.1109/TAC.1974.1100705

Andreasson, A., Jönsson, B., Lindman, B.J.C. and Science, P., 1988. Surface and colloid chemistry of peat and peat dewatering. Electrostatic effects. 266(2): 164-172.http://dx.doi.org/10.1007/bf01452814

Appelo, C.A.J. and Postma, D., 2005. Geochemistry, Groundwater and pollution. A.A. Balkema Publihers, Leiden, The Netherlands.

Baird, A.J. and Gaffney, S.W., 2000. Solute movement in drained fen peat: a field tracer study in a Somerset (UK) wetland. Hydrological Processes, 14(14): 2489-2503.http://dx.doi.org/10.1002/1099-1085(20001015)14:14<2489::aid-hyp110>3.0.co;2-q

Balliston, N.E., McCarter, C.P.R. and Price, J.S., 2018. Microtopographical and hydrophysical controls on subsurface flow and solute transport: A continuous solute release experiment in a subarctic bog. 32(19): 2963-2975.http://dx.doi.org/10.1002/hyp.13236

Bates, D., Maechler, M., Bolker, B. and Walker, S., 2015. Fitting Linear Mixed-Effects Models Using lme4. Journal of Statistical Software, 67(1): 1-48.http://10.18637/jss.v067.i01

Boudreau, J., Caron, J., Elrick, D., Fortin, J. and Gallichand, J., 2009. Solute transport in sub-irrigated peat-based growing media. Canadian Journal of Soil Science, 89(3): 301-313.http://dx.doi.org/10.4141/cjss08023

Bradford, S.A., Simunek, J., Bettahar, M., van Genuchten, M.T. and Yates, S.R., 2003. Modeling Colloid Attachment, Straining, and Exclusion in Saturated Porous Media. Environmental Science & Technology, 37(10): 2242-2250.https://doi.org/10.1021/es025899u

Bratskaya, S., Golikov, A., Lutsenko, T., Nesterova, O. and Dudarchik, V., 2008. Charge characteristics of humic and fulvic acids: Comparative analysis by colloid titration and potentiometric titration with continuous pK-distribution function model. Chemosphere, 73(4): 557-563.https://doi.org/10.1016/j.chemosphere.2008.06.014

Bresler, E., 1973. Anion Exclusion and Coupling Effects in Nonsteady Transport Through Unsaturated Soils: I. Theory1. 37(5): 663-669.http://doi.org/10.2136/sssaj1973.03615995003700050013x

Carey, S.K., Quinton, W. and Goeller, N.T., 2007. Field and laboratory estimates of pore size properties and hydraulic characteristics for subarctic organic soils. Hydrological Processes, 21: 2560-2571.http://dx.doi.org/10.1002/hyp.6795

Caron, J., Létourneau, G. and Fortin, J., 2015. Electrical conductivity breakthrough experiment and immobile water estimation in organic substrates: Is R = 1 a realistic assumption? Vadose Zone Journal, 14(9).http://dx.doi.org/10.2136/vzj2015.01.0014

Cohen, A.D., Rollins, M.S., Zunic, W.M. and Durig, J.R., 1991. Effects of chemical and physical differences in peats on their ability to extract hydrocarbons from water. Water Research, 25(9): 1047-1060.https://doi.org/10.1016/0043-1354(91)90198-Y

Comas, X. and Slater, L., 2004. Low-frequency electrical properties of peat. Water Resources Research, 40(12): n/a-n/a.http://dx.doi.org/10.1029/2004WR003534

Delicato, D.M.S., 1996. Physical-Chemical Properties and Sorption Characteristics of Peat, Dublin Citiy University, Dublin, Ireland.

ACCEPTED MANUSCRIPT

Easteal, A.J., Edge, A.V.J. and Woolf, L.A., 1984. Isotope effects in water. Tracer diffusion coefficients for water(oxygen-18) (H218O) in ordinary water. The Journal of Physical Chemistry, 88(24): 6060-6063.https://doi.org/10.1021/j150668a065

Gharedaghloo, B., 2018. Characterizing the transport of hydrocarbon contaminants in peat soils and peatlands, University of Waterloo, UWSpace.

Gharedaghloo, B. and Price, J.S., 2017. Fate and transport of free-phase and dissolved-phase hydrocarbons in peat and peatlands: developing a conceptual model. Environmental Reviews, 26(1): 55-68.http://dx.doi.org/10.1139/er-2017-0002

Gharedaghloo, B. and Price, J.S., 2018. Characterizing the immiscible transport properties of diesel and water in peat soil. Journal of Contaminant Hydrology.https://doi.org/10.1016/j.jconhyd.2018.12.005

Gharedaghloo, B., Price, J.S., Rezanezhad, F. and Quinton, W.L., 2018. Evaluating the hydraulic and transport properties of peat soil using pore network modeling and X-ray micro computed tomography. Journal of Hydrology, 561: 494-508.https://doi.org/10.1016/j.jhydrol.2018.04.007

Glaser, P.H., Siegel, D.I., Romanowicz, E.A. and Shen, Y.P., 1997. Regional Linkages Between Raised Bogs and the Climate, Groundwater, and Landscape of North-Western Minnesota. Journal of Ecology, 85(1): 3-16.http://dx.doi.org/10.2307/2960623

Gogo, S., Shreeve, T.G. and Pearce, D.M.E., 2010. Geochemistry of three contrasting British peatlands: Complex patterns of cation availability and impications for microbial metabolism. Geoderma, 158: 207-215.http://dx.doi.org/10.1016/j.geoderma.2010.04.031

Gondar, D., Lopez, R., Fiol, S., Antelo, J.M. and Arce, F., 2005a. Characterization and acid–base properties of fulvic and humic acids isolated from two horizons of an ombrotrophic peat bog. Geoderma, 126(3): 367-374.https://doi.org/10.1016/j.geoderma.2004.10.006

Gondar, D., López, R., Fiol, S., Antelo, J.M. and Arce, F., 2005b. Effect of soil depth on acid properties of humic substances extracted from an ombrotrophic peat bog in northwest Spain. 56(6): 793-801.https://doi.org/10.1111/j.1365-2389.2005.00715.x

Graniero, P.A., 1999. The effect of spatiotemporal sampling strategies and data acquisition accuracy on the characterization of a dynamic ecological system, 18th International Conference of the North American Fuzzy Information Processing Society - NAFIPS (Cat. No.99TH8397), pp. 829-833.

Gvirtzman, H. and Gorelick, S.M., 1991. Dispersion and advection in unsaturated porous media enhanced by anion exclusion. Nature, 352: 793.https://doi.org/10.1038/352793a0

Hayward, P.M. and Clymo, R.S., 1982. Profiles of water content and pore size in *Sphagnum* and peat, and their relation to peat bog ecology. Proceedings of the Royal Society B: Biological Sciences, 215: 299-325.

Ho, Y.S. and McKay, G., 1999. Competitive sorption of copper and nickel ions from aqueous solution using peat. Adsorption, 5(4): 409-417.http://dx.doi.org/10.1023/a:1008921002014

Ho, Y.S., Porter, J.F. and McKay, G., 2002. Equilibrium isotherm studies for the sorption of divalent metal ions onto peat: copper, nickel and lead single component systems. Water, Air, and Soil Pollution, 141(1): 1-33.http://dx.doi.org/10.1023/a:1021304828010

Hoag, R.S. and Price, J.S., 1995. A field-scale, natural gradient solute transport experiment in peat at a Newfoundland blanket bog. Journal of Hydrology, 172: 171-184.https://doi.org/10.1016/0022-1694(95)02696-M

ACCEPTED MANUSCRIPT

Hoag, R.S. and Price, J.S., 1997. Effects of matrix diffusion on solute transport and retardation peat. Journal of Contaminant Hydrology, 28: 193-205.https://doi.org/10.1016/S0169-7722(96)00085-X

Huysmans, M. and Dassargues, A.J.H.J., 2005. Review of the use of Péclet numbers to determine the relative importance of advection and diffusion in low permeability environments. 13(5): 895-904.https://doi.org/10.1007/s10040-004-0387-4

James, R.V. and Rubin, J., 1986. Transport of Chloride Ion in a Water-unsaturated Soil Exhibiting Anion Exclusion1. 50(5): 1142-1149.https://doi.org/10.2136/sssaj1986.03615995005000050010x

Kennedy, G. and Price, J., 2005. A conceptual model of volume-change controls on the hydrology of cutover peats. Journal of Hydrology, 302: 13-27.https://doi.org/10.1016/j.jhydrol.2004.06.024

Kettridge, N. and Binley, A., 2010. Evaluating the effect of using artificial pore water on the quality of laboratory hydraulic conductivity measurements of peat. Hydrological Processes, 24(18): 2629-2640.http://dx.doi.org/10.1002/hyp.7693

Kleimeier, C., Karsten, U. and Lennartz, B., 2014. Suitability of degraded peat for constructed wetlands — Hydraulic properties and nutrient flushing. Geoderma, 228–229: 25-32.http://dx.doi.org/10.1016/j.geoderma.2013.12.026

Kleimeier, C., Rezanezhad, F., Van Cappellen, P. and Lennartz, B., 2017. Influence of pore structure on solute transport in degraded and undegraded fen peat soil. Mires and Peat, 19(18): 1-9.http://dx.doi.org/10.19189/MaP.2017.OMB.282

Koeniger, P., Leibungut, C., Link, T. and Marshall, J.D., 2010. Stable isotopes applied as water tracers in column and field studies. Organic Geochemistry, 41: 31-40.https://doi.org/10.1016/j.orggeochem.2009.07.006

Lenth, R.V., 2016. Least-Squares Means: The R Package lsmeans. Journal of Statistical Software, 69(1): 1-33.http://10.18637/jss.v069.i01

Lewis, J. and Sjöstrom, J., 2010. Optimizing the experimental design of soil columns in saturated and unsaturated transport experiments. Journal of Contaminant Hydrology, 115(1–4): 1-13.http://dx.doi.org/10.1016/j.jconhyd.2010.04.001

Limousin, G., Gaudet, J.P., Charlet, L., Szenknect, S., Barthès, V. and Krimissa, M., 2007. Sorption isotherms: A review on physical bases, modeling and measurement. Applied Geochemistry, 22(2): 249-275.https://doi.org/10.1016/j.apgeochem.2006.09.010

Liu, H., Forsmann, D.M., Kjærgaard, C., Saki, H. and Lennartz, B., 2017. Solute Transport Properties of Fen Peat Differing in Organic Matter Content. Journal of Environmental Quality.http://dx.doi.org/10.2134/jeq2017.01.0031

Liu, H., Janssen, M. and Lennartz, B., 2016. Changes in flow and transport patterns in fen peat following soil degradation. European Journal of Soil Science, 67(6): 763-772.https://doi.org/10.1111/ejss.12380

McCarter, C.P.R., Branfireun, B.A. and Price, J.S., 2017a. Nutrient and mercury transport in a sub-arctic ladder fen peatland subjected to simulated wastewater discharges. Science of The Total Environment, 609(Supplement C): 1349-1360.https://doi.org/10.1016/j.scitotenv.2017.07.225

McCarter, C.P.R., Ketcheson, S., Weber, T.K.D., Whittington, P., Scarlett, S. and Price, J., 2017b. Modified Technique for Measuring Unsaturated Hydraulic Conductivity in Sphagnum Moss and Peat. Soil Science Society of America Journal, 81(4): 747-757.http://dx.doi.org/10.2136/sssaj2017.01.0006

ACCEPTED MANUSCRIPT

McCarter, C.P.R. and Price, J.S., 2014. Ecohydrology of *Sphagnum* moss hummocks: mechanisms of capitula water supply and simulated effects of evaporation. Ecohydrology, 7(1): 33-44.http://dx.doi.org/10.1002/eco.1313

McCarter, C.P.R. and Price, J.S., 2017. The transport dynamics of chloride and sodium in a ladder fen during a continuous wastewater polishing experiment. Journal of Hydrology, 549: 558-570.http://dx.doi.org/10.1016/j.jhydrol.2017.04.033

McCarter, C.P.R., Weber, T.K.D. and Price, J.S., 2018. Competitive transport processes of chloride, sodium, potassium, and ammonium in fen peat. Journal of Contaminant Hydrology, 217: 17-31.http://doi.org/10.1016/j.jconhyd.2018.08.004

Mualem, Y., 1976. A new model for predicting the hydraulic conductivity of unsaturated porous media. Water Resources Research, 12: 513-522.

Murday, J.S. and Cotts, R.M., 1970. Self- Diffusion in Liquids: H2O, D2O, and Na. The Journal of Chemical Physics, 53(12): 4724-4725.https://doi.org/10.1063/1.1674011

Ours, D., Siegel, D.I. and Glaser, P.H., 1997. Chemical dilation and the dual porosity of humified bog peat. Journal of Hydrology, 196: 348-360.http://doi.org/10.1016/S0022-1694(96)03247-7

Pallud, C., Meile, C., Laverman, A.M., Abell, J. and Van Cappellen, P., 2007. The use of flow-through sediment reactors in biogeochemical kinetics: Methodology and examples of applications. Marine Chemistry, 106(1–2): 256-271.http://dx.doi.org/10.1016/j.marchem.2006.12.011

Pinheiro, J., Bates, D., DebRoy, S. and Team, R.D.C., 2018. nlme: Linear and Nonlinear Mixed Effects Models.

Quinton, W.L., Elliot, T., Price, J.S., Rezanezhad, F. and Heck, R., 2009. Measuring physical and hydraulic properties of peat from X-ray tomography. Geoderma, 153: 269-277.https://doi.org/10.1016/j.geoderma.2009.08.010

R Development Core Team, 2018. R: A language and environment for statistical computing. R Foundation for Statistitical Computing, Vienna, Austria.

Rajendran, A., Kariwala, V. and Farooq, S., 2008. Correction procedures for extra-column effects in dynamic column breakthrough experiments. Chemical Engineering Science, 63(10): 2696-2706.https://doi.org/10.1016/j.ces.2008.02.023

Redding, T.E. and Devito, K.J., 2006. Particle densities of wetland soils in northern Alberta, Canada. Canadian Journal of Soil Science, 86(1): 57-60.http://dx.doi.org/10.4141/S05-061

Rezanezhad, F., Kleimeier, C., Milojevic, T., Liu, H., Weber, T.K.D., Van Cappellen, P. and Lennartz, B., 2017. The Role of Pore Structure on Nitrate Reduction in Peat Soil: A Physical Characterization of Pore Distribution and Solute Transport. Wetlands, 37(5): 951-960.http://dx.doi.org/10.1007/s13157-017-0930-4

Rezanezhad, F., Price, J.S. and Craig, J.R., 2012. The effects of dual porosity on transport and retardation in peat: A laboratory experiment. Canadian Journal of Soil Science, 92(5): 723-732.http://dx.doi.org/10.4141/cjss2011-050

Rezanezhad, F., Price, J.S., Quinton, W.L., Lennartz, B., Milojevic, T. and Van Cappellen, P., 2016. Structure of peat soils and implications for water storage, flow and solute transport: A review update for geochemists. Chemical Geology, 429: 75-84.http://dx.doi.org/10.1016/j.chemgeo.2016.03.010

Rezanezhad, F., Quinton, W.L., Price, J.S., Elliot, T.R., Elrick, D. and Shook, K.R., 2010. Influence of pore size and geometry on peat unsaturated hydraulic conductivity computed

ACCEPTED MANUSCRIPT

from 3D computed tomography image analysis. Hydrological Processes, 2994: 2983-2994. https://doi.org/10.1002/hyp.7709

Richter, C. and Dainty, J., 1989. Ion behavior in plant cell walls. II. Measurement of the Donnan free space, anion-exclusion space, anion-exchange capacity, and cation-exchange capacity in delignified Sphagnum russowii cell walls. Canadian Journal of Botany, 67(2): 460-465.https://doi.org/10.1139/b89-064

Rippy, J.F.M. and Nelson, P.V., 2007. Cation Exchange Capacity and Base Saturation Variation among Alberta, Canada, Moss Peats. HortScience, 42(2): 349-352.

Rose, D.A., Abbas, F. and Adey, M.A., 2009. The effect of surface–solute interactions on the transport of solutes through porous materials. 60(3): 398-411.https://doi.org/10.1111/j.1365-2389.2009.01122.x

Rutherford, D.W., Chiou, C.T. and Kile, D.E., 1992. Influence of soil organic matter composition on the partition of organic compounds. Environmental Science & Technology, 26(2): 336-340.https://doi.org/10.1021/es00026a014

Sauer, P.E., Schimmelmann, A., Sessions, A.L. and Topalov, K., 2009. Simplified batch equilibration for D/H determination of non-exchangeable hydrogen in solid organic material. Rapid Communications in Mass Spectrometry, 23(7): 949-956.https://doi.org/10.1002/rcm.3954

Schimmelmann, A., 1991. Determination of the concentration and stable isotopic composition of nonexchangeable hydrogen in organic matter. Analytical Chemistry, 63(21): 2456-2459.https://doi.org/10.1021/ac00021a013

Shimizu, S., 2014. fitAdsorptionIsotherm, MATLab.

Simhayov, R.B., Weber, T.K.D. and Price, J.S., 2018. Saturated and unsaturated salt transport in peat from a constructed fen. SOIL, 4: 63-81.https://doi.org/10.5194/soil-4-63-2018

Šimůnek, J., Jarvis, N.J., van Genuchten, M. and Gärdenäs, A., 2003. Review and comparison of models for describing non-equilibrium and preferential flow and transport in the vadose zone. Journal of Hydrology, 272: 14-35.https://doi.org/10.1016/S0022-1694(02)00252-4

Šimůnek, J., Šejna, M., Saito, H., Sakai, M. and van Genuchten, M.T., 2008. The Hydrus-1D Software Package for Simulating the Movement of Water, Heat, and Multiple Solutes in Variably Saturated Media, Hydrus Series. Department of Environmental Sciences, University of California Riverside, Riverside, CA, USA.

Šimůnek, J. and van Genuchten, M.T., 2008. Modeling Nonequilibrium Flow and Transport Processes Using HYDRUS. Vadose Zone Journal, 7(2): 782-797.https://doi.org/10.2136/vzj2007.0074

Sips, R., 1948. On the Structure of a Catalyst Surface. The Journal of Chemical Physics, 16(5): 490-495.https://doi.org/10.1063/1.1746922

Smith, D., Pivonka, P., Jungnickel, C. and Fityus, S., 2004. Theoretical Analysis of Anion Exclusion and Diffusive Transport Through Platy-Clay Soils. Transport in Porous Media, 57(3): 251-277.http://dx.doi.org/10.1007/s11242-003-4056-1

van Genuchten, M., 1980. A closed-form equation for predicting the hydraulic conductivity of unsaturated soils. Soil Science Society of America Journal, 44: 892-898.

Van Loon, L.R., Glaus, M.A. and Müller, W., 2007. Anion exclusion effects in compacted bentonites: Towards a better understanding of anion diffusion. Applied Geochemistry, 22(11): 2536-2552.https://doi.org/10.1016/j.apgeochem.2007.07.008

ACCEPTED MANUSCRIPT

Vanderborght, J., Mallants, D., Vanclooster, M. and Feyen, J., 1997. Parameter uncertainty in the mobile-immobile solute transport model. Journal of Hydrology, 190(1): 75-101.https://doi.org/10.1016/S0022-1694(96)03064-8

von Post, L., 1926. Södra Sveriges Torvtillgånger, I. Sver.Geo.Unders., C35(19 (2)).

Weber, T.K.D., Iden, S.C. and Durner, W., 2017. Unsaturated hydraulic properties of *Sphagnum* moss and peat reveal trimodal pore-size distributions. Water Resources Research, 53(1): 415-434.http://dx.doi.org/10.1002/2016WR019707

Wehrer, M. and Totsche, K.U., 2005. Determination of effective release rates of polycyclic aromatic hydrocarbons and dissolved organic carbon by column outflow experiments. 56(6): 803-813.https://doi.org/10.1111/j.1365-2389.2005.00716.x

ACCEPTED MANUSCRIPT

ACCEPTED MANUSCRIPT

Figure Captions

Figure 1: Equilibrium Cl- adsorption isotherms for each peat type. Two separate batch experiments (Batch 1 and Batch 2), with triplicate replicates in each batch experiment, were preformed. Note, both axes are log transformed.

Figure 2: BTCs for deuterium (black) and Cl^- assuming anion exclusion (grey) for each sample. Only the Cl^- assuming anion exclusion is displayed as there was no distinguishable difference in modelled lines between the Cl^- methods. Note, the parameters and measures of fit for each BTC are shown in Table 3, Table S2, Table S3, and Table 7.

Figure 3: Measured, as determined by the drainable porosity at -100 mb, and estimated mobile porosity with 1:1 line. Note, below the 1:1 line suggests a decrease in mobile porosity, while above the 1:1 line an increase.

Figure 4: 1:1 plots of the estimated parameters using Cl^- relative to those determined by deuterated water. Note, good agreement between tracers was achieved when the points fall along the 1:1 line.

Figure 5: Measured and modelled Cl^- BTCs assuming and not assuming anion exclusion and using the hydrophysical parameters (λ and θ_{im}) determined by the deuterated water tracer. The MiM parameters for each curve can be found in Table 6.

ACCEPTED MANUSCRIPT

ACCEPTED MANUSCRIPT

Table 1: The total porosity (ϕ), effective porosity (n_e) and bulk density (ρ) used in the mobile-immobile model for each core

	ϕ	n_e	ρ
	[-]	[-]	[g cm^{-3}]
Undecomposed 1	0.97	0.38	0.05
Undecomposed 2	0.96	0.29	0.05
Undecomposed 3	0.95	0.34	0.06
Decomposed 1	0.95	0.45	0.08
Decomposed 2	0.93	0.28	0.12
Decomposed 3	0.93	0.16	0.10

Table 2: The Freundlich isotherm constant (K_F) and exponent (N), along with measure of fit determined from the equilibrium batch experiments.

	K_F	N	RMSE	R^2
	mg^{1-N} g^{-1} mL^N	[-]	[mg g^{-1}]	[-]
H1 – 1	61.25	2.26	8.39	0.92
H1 – 2	0.37	0.94	0.19	0.75
H4 – 1	1.17	1.13	3.10	1.00
H4 – 2	1.97	0.92	0.16	0.99
H7 – 1	0.33	0.12	0.23	0.81
H7 – 2	49.29	1.41	7.80	0.73
Milled – 1	12.92	1.04	15.50	1.00
Milled – 2	2.12	0.89	0.53	0.82

Table 3: Average (± 95% C.I.) HDO BTC determined dispersivity (λ_{2H}), immobile pore region ($\theta_{im\ 2H}$), first-order mass transfer coefficient ($\omega_{mim\ 2H}$), and measures of fit for each sample (n = 20).

	λ_{2H}	$\theta_{im\ 2H}$	$\alpha_{mim\ 2H}$	ω_{2H}	Pe_{2H}	Da_{2H}	RMSE	AIC
	[cm]	[-]	[day^{-1}]	[-]	[-]	[-]	[-]	[-]
Undecomposed 1	0.17 ± 0.03	0.60 ± 0.02	5.0 ± 0.6	9.7	62	3.5	0.021	60
Undecomposed 2	0.25 ± 0.03	0.66 ± 0.02	24.4 ± 8.8	46.8	73	14.5	0.050	55
Undecomposed 3	0.22 ± 0.03	0.60 ± 0.02	16.2 ± 2.8	31.2	65	10.9	0.039	72
Decomposed 1	0.53 ± 0.09	0.49 ± 0.03	1.7 ± 0.3	3.2	50	1.5	0.032	100
Decomposed 2	0.63 ± 0.02	0.57 ± 0.03	54.3 ± 10.7	104.4	78	30.4	0.041	60
Decomposed 3	0.58 ± 0.04	0.77 ± 0.03	47.6 ± 13.6	91.6	144	14.4	0.044	54

ACCEPTED MANUSCRIPT

Table 4: Average (± 95% C.I.) Cl^- BTC with anion exclusion determined dispersivity ($\lambda_{Cl\,AE}$), immobile pore region ($\theta_{im\,Cl\,AE}$), first-order mass transfer coefficient ($\omega_{mim\,Cl\,AE}$), linear partitioning coefficient ($Kd_{Cl\,AE}$) and measures of fit for each sample.

	$\lambda_{Cl\,AE}$	$\theta_{im\,Cl\,AE}$	$\alpha_{mim\,Cl\,AE}$	$\omega_{Cl\,AE}$	$Kd_{Cl\,AE}$	$Pe_{Cl\,AE}$	$Da_{Cl\,AE}$	$\phi_{ex\,AE}$	R	RMSE	AIC
	[cm]	[-]	[day^{-1}]	[-]		[-]	[-]	[-]	[-]	[-]	[-]
Undecomposed 1	0.26 ± 0.07	0.60 ± 0.02	4.6 ± 1.3	8.9	-0.54 ± 0.14	78	3.3	0.01	0.97	0.038	94
Undecomposed 2	0.37 ± 0.06	0.67 ± 0.03	36.5 ± 11.1	70.2	-0.97 ± 0.19	99	21.9	0.01	0.95	0.081	105
Undecomposed 3	0.34 ± 0.05	0.62 ± 0.03	46.8 ± 13.6	90.0	-1.09 ± 0.11	86	32.6	0.02	0.93	0.024	90
Decomposed 1	0.67 ± 0.20	0.50 ± 0.02	1.2 ± 0.20	2.2	-0.66 ± 0.19	65	1.0	0.02	0.95	0.033	97
Decomposed 2	0.46 ± 0.08	0.65 ± 0.02	32.3 ± 9.1	62.2	-1.34 ± 0.07	107	15.5	0.05	0.83	0.058	100
Decomposed 3	0.61 ± 0.10	0.73 ± 0.02	26.5 ± 7.2	51.0	-1.13 ± 0.13	146	17.3	0.02	0.88	0.073	92

Table 5: The resultant p-values of the estimated pair-wise comparison between individual fitting methods for all physical parameters. Cl^- no ADS is Cl^- without accounting for adsorption and Cl^- ADS is Cl^- with accounting for adsorption. Note, θ_{mo} and v_{mo} were replaced with θ_{eff} and v_{eff} in the anion exclusion case.

Interaction	λ	D_{mo}	θ_{im}	θ_{mo}	v_{mo}
HDO-Cl^- ADS	<0.0001	<0.0001	0.56	0.56	0.50
HDO-Cl^- no ADS	<0.0001	<0.0001	0.81	0.81	0.54
HDO-Cl^- AE	0.27	0.79	0.97	0.0002	0.66
Cl^- ADS-Cl^- no ADS	0.77	0.16	0.12	0.12	0.032
Cl^- ADS-Cl^- AE	<0.0001	<0.0001	0.30	<0.0001	0.055
Cl^- no ADS- Cl^- AE	<0.0001	<0.0001	0.97	0.0065	1.00

Table 6: Average (± 95% C.I.) Cl^- BTC using physical parameters determined by deuterated water. Note, only $\omega_{mim\,Cl-HDO}$ and $Kd_{Cl\,2H}$ were fit in this simulation and Da_{Cl} and R calculated.

	λ_{2H}	$\theta_{im\,2H}$	$\alpha_{mim\,Cl\,HDO}$	$\omega_{Cl\,HDO}$	$Kd_{Cl\,HDO}$	R	$Pe_{Cl\,HDO}$	$Da_{Cl\,HDO}$	ϕ_{ex}	RMSE	AIC
	[cm]	[-]	[day^{-1}]	[-]	[mL g^{-1}]	[-]	[-]	[-]	[-]	[-]	[-]
Undecomposed 1	0.17	0.60	2.9 ± 0.1	5.57	-0.28 ± 0.07	0.99	79	2.0	0.00	0.032	93
Undecomposed 2	0.25	0.66	15.5 ± 1.7	29.85	-1.26 ± 0.06	0.94	94	9.2	0.02	0.080	102
Undecomposed 3	0.22	0.60	15.4 ± 1.5	29.65	-1.32 ± 0.08	0.91	82	10.4	0.03	0.024	88
Decomposed 1	0.53	0.49	1.0 ± 0.11	2.00	-0.82 ± 0.20	0.93	64	0.9	0.03	0.032	99
Decomposed 2	0.63	0.57	57.5 ± 10.0	110.58	-1.30 ± 0.06	0.84	99	32.2	0.05	0.056	95
Decomposed 3	0.58	0.77	28.5 ± 3.0	54.83	-1.28 ± 0.03	0.86	183	8.6	0.02	0.068	89

ACCEPTED MANUSCRIPT

Table 7: The resultant p-values of the estimated pair-wise comparison of α_{mim} between tracers and decomposition state.

Interaction	Decomposed HDO	Undecomposed HDO	Decomposed Cl^-	Undecomposed Cl^-
Decomposed HDO –				
Undecomposed HDO	<0.0001			
Decomposed Cl^-	0.54	0.0049		
Undecomposed Cl^-	<0.0001	0.78	<0.0001	

Table 8: The ratios between ω_{mim} values of the HDO and Cl^- using physical parameters determined by deuterated water. Averages are presented, along with the 95 % confidence interval based on n = 3.

	$\alpha_{mim\ 2H}$	$\alpha_{mim\ Cl\ HDO}$	$\alpha_{mim\ 2H} / \alpha_{mim\ Cl\ HDO}$	Avg.
	[day^{-1}]	[day^{-1}]	[-]	[-]
Undecomposed 1	5.0 ± 0.6	2.9 ± 0.1	0.58	0.74 ± 0.16
Undecomposed 2	24.4 ± 8.8	15.5 ± 1.7	0.64	
Undecomposed 3	16.2 ± 2.8	15.4 ± 1.5	0.95	
Decomposed 1	1.7 ± 0.3	1.0 ± 0.11	0.62	0.84 ± 0.24
Decomposed 2	54.3 ± 10.7	57.5 ± 10.0	1.06	
Decomposed 3	47.6 ± 13.6	28.5 ± 3.0	0.60	

ACCEPTED MANUSCRIPT

ACCEPTED MANUSCRIPT

Table S1: Upper and lower bounds of the global fitting parameters: dispersivity (λ), immobile pore region (θ_{im}), first-order mass transfer coefficient (ω_{mim}), fraction of adsorption sites that equilibrate in the mobile region (f_{mo}), Freundlich isotherm parameters ($K_{F\,mim}$ and N_{mim}). The Freundlich isotherm parameters and f_{mo} were set to 0, 1, and 1 for $K_{F\,mim}$ and N_{mim} and f_{mo} when not accounting for adsorption in the BTC analysis. * indicates a log scale was used to normalize the distribution in the global search function.

	λ *		θ_{im}		f_{mo}		$K_{F\,mim}$ *		N_{mim} *		ω_{mim} *		Kd	
	min	max	min	max	min	max	min	max	min	max	min	max	min	max
bound	0.1	10	n_e	$\pm$ 0.1	0.01	0.99	0.001	10	0.1	10	0.1	100	-2.0	0.0

Table S2: Average (± 95% C.I.) Cl^- BTC without adsorption determined dispersivity (λ_{Cl}), immobile pore region ($\theta_{im\,Cl}$), first-order mass transfer coefficient ($\omega_{mim\,Cl}$), and measures of fit for each sample.

	λ_{Cl}	$\theta_{im\,Cl}$	$\alpha_{mim\,Cl}$	ω_{Cl}	Pe_{Cl}	Da_{Cl}	RMSE	AIC
	[cm]	[-]	[day^{-1}]	[-]	[-]	[-]	[-]	[-]
Undecomposed 1	0.34 ± 0.06	0.60 ± 0.03	4.5 ± 0.8	8.7	79	3.2	0.034	94
Undecomposed 2	0.55 ± 0.08	0.65 ± 0.02	42.6 ± 9.9	81.9	92	25.6	0.082	107
Undecomposed 3	0.57 ± 0.02	0.59 ± 0.02	60.8 ± 9.0	117.0	80	42.3	0.038	89
Decomposed 1	0.97 ± 0.25	0.49 ± 0.02	1.17 ± 0.26	2.3	64	1.0	0.032	95
Decomposed 2	1.51 ± 0.09	0.67 ± 0.03	48.3 ± 11.0	92.9	116	23.1	0.088	88
Decomposed 3	1.36 ± 0.07	0.79 ± 0.02	45.5 ± 8.4	87.4	201	12.6	0.075	87

ACCEPTED MANUSCRIPT

ACCEPTED MANUSCRIPT

Table S3: Average (± 95% C.I.) Cl^- BTC with adsorption determined dispersivity (λ_{Cl-ads}), immobile pore region ($\theta_{im\ Cl-ads}$), first-order mass transfer coefficient ($\omega_{mim\ Cl-ads}$), fraction of adsorption sites that equilibrate in the mobile region (f_{mo}), Freundlich isotherm parameters ($K_{F\,mim}$ and N_{mim}), and measures of fit for each sample.

	λ_{Cl-ads}	$\theta_{im\ Cl-ads}$	$\alpha_{mim\ Cl-ads}$	f_{mo}	$K_{F\,mim}$	N_{mim}	RMSE	AIC
	[cm]	[-]	[day^{-1}]	[-]	mg^{1-N} g^{-1} mL^{N}	[-]	[-]	[-]
Undecomposed 1	0.21 ± 0.02	0.54 ± 0.02	2.5 ± 0.3	0.60 ± 0.12	1.3 ± 0.9	17.1 ± 7.8	0.031	104
Undecomposed 2	0.59 ± 0.03	0.66 ± 0.02	62.9 ± 7.45	0.47 ± 0.11	1.6 ± 1.0	27.6 ± 13.1	0.081	110
Undecomposed 3	0.62 ± 0.02	0.57 ± 0.02	70.0 ± 8.0	0.50 ± 0.13	2.0 ± 1.2	21.2 ± 11.8	0.036	98
Decomposed 1	1.23 ± 0.16	0.52 ± 0.02	1.6 ± 0.3	0.48 ± 0.13	2.0 ± 0.9	16.8 ± 10.8	0.030	112
Decomposed 2	1.52 ± 0.07	0.64 ± 0.02	60.7 ± 9.0	0.51 ± 0.12	3.2 ± 1.4	28.4 ± 9.4	0.080	98
Decomposed 3	1.29 ± 0.05	0.76 ± 0.02	66.1 ± 10.0	0.44 ± 0.12	2.4 ± 1.2	19.7 ± 7.6	0.076	97

Table S4: The fixed effects least-squares means and the upper and lower 95% confidence intervals of the Mixed Effect Models comparing HDO and Cl^- tracers. Cl^- no ADS is Cl^- without accounting for adsorption and Cl^- ADS is Cl^- with accounting for adsorption.

Method	λ	D_{mo}	θ_{im}	θ_{mo}	v_{mo}
	LS-mean (upper, lower C.I.)	LS-mean (upper, lower C.I.)	LS-mean (upper, lower C.I.)	LS-mean (upper, lower C.I.)	LS-mean (upper, lower C.I.)
HDO	0.39 (0.00, 0.80)	8.3 (0.0, 23.1)	0.32 (0.21, 0.43)	0.63 (0.53, 0.72)	19.3 (9.3, 29.2)
Cl^- no ADS	0.88 (0.48, 1.29)	20.8 (5.9, 35.7)	0.32 (0.21, 0.42)	0.63 (0.54, 0.73)	20.4 (10.4, 30.4)
Cl^- ADS	0.88 (0.48, 1.29)	18.3 (3.4, 33.1)	0.33 (0.21, 0.42)	0.62 (0.52, 0.71)	18.1 (8.1, 28.1)

Table S5: Average (± 95% C.I.) Cl^- BTC using physical parameters determined by deuterated water without anion exclusion. Note, only $\omega_{mim\ NAE}$ were fit in this simulation and Da_{Cl} calculated.

	λ_{2H}	$\theta_{im\ 2H}$	$\alpha_{mim\ NAE}$	ω_{NAE}	Pe_{NAE}	Da_{NAE}	RMSE	AIC
	[cm]	[-]	[day^{-1}]	[-]	[-]	[-]	[-]	[-]
Undecomposed 1	0.17	0.60	2.7 ± 0.06	5	79	2	0.033	88
Undecomposed 2	0.25	0.66	91.3 ± 2.36	176	94	54	0.101	90
Undecomposed 3	0.22	0.60	8.3 ± 0.13	16.0	82	6	0.066	85
Decomposed 1	0.53	0.49	2.8 ± 0.06	5.4	64	2	0.097	84
Decomposed 2	0.63	0.57	90.5 ± 2.67	174	99	51	0.131	82
Decomposed 3	0.58	0.77	90.6 ± 2.43	174	183	27	0.144	79

ACCEPTED MANUSCRIPT

Table S6: The fixed effects least-squares means and the upper and lower 95% confidence intervals of the Mixed Effect Models comparing diffusion parameters determined by the Cl^- with λ_{2H} and $\theta_{im\ 2H}$.

Decomposition Level	$\alpha_{mim\ 2H}$	$\alpha_{mim\ Cl-2H}$
	LS-mean (upper, lower C.I.)	LS-mean (upper, lower C.I.)
Undecomposed	15.2 (10.6, 19.8)	11.3 (5.5, 17.0)
Decomposed	34.5 (29.9, 39.1)	23.3 (23.3, 34.8)

ACCEPTED MANUSCRIPT

ACCEPTED MANUSCRIPT

Highlights

5. Chloride is not, strictly speaking, a conservative tracer
6. Chloride sorbs to peat, but the extent of binding is low and highly variable
7. Anion exclusion was observed but it did not appreciably affect chloride breakthrough
8. Chloride diffusion into immobile porosity is not governed by degree of decomposition

ACCEPTED MANUSCRIPT

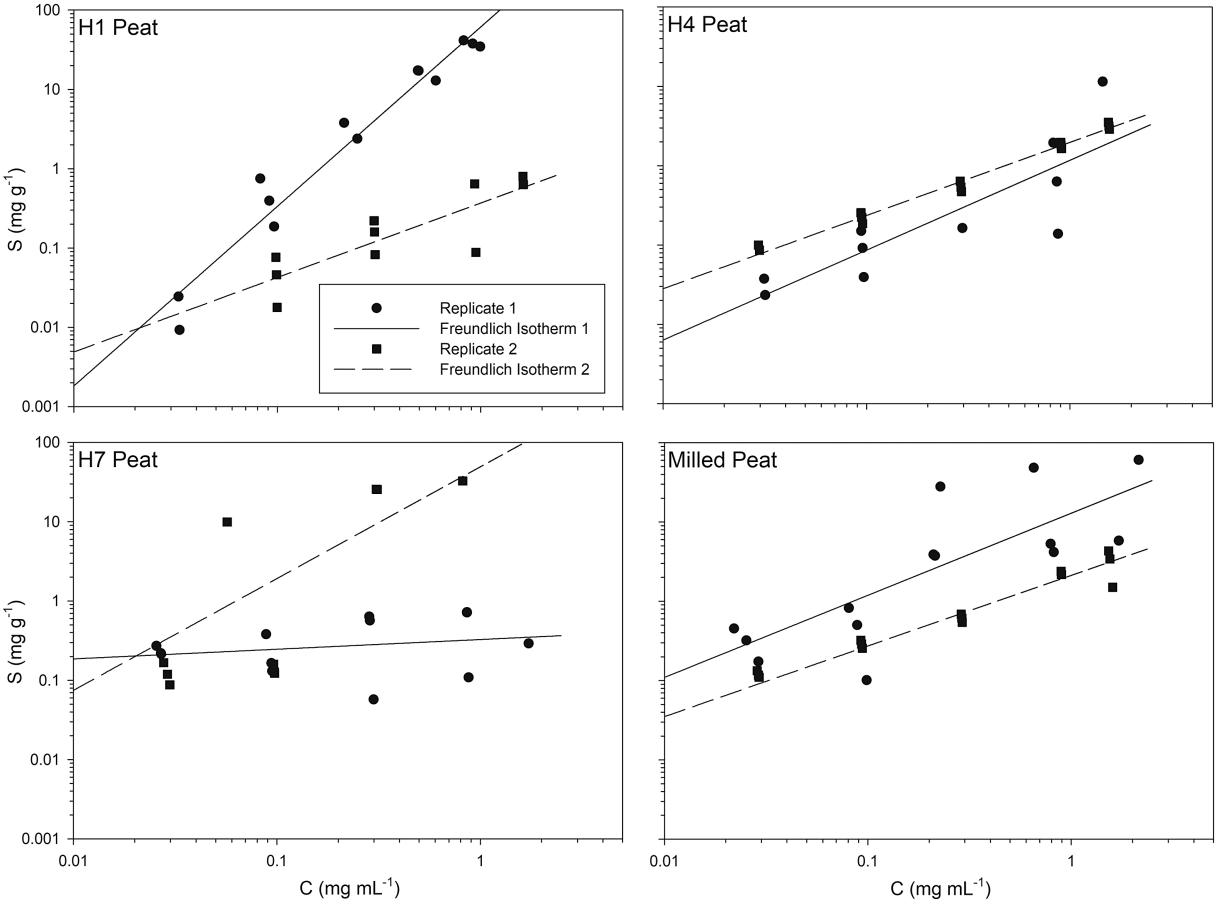
H1 Peat
H4 Peat
H7 Peat
Milled Peat
S (mg g-1)
C (mg mL-1)
Replicate 1
Freundlich Isotherm 1
Replicate 2
Freundlich Isotherm 2
100
10
1
0.1
0.01
0.001
0.01
0.1
1

Figure 1

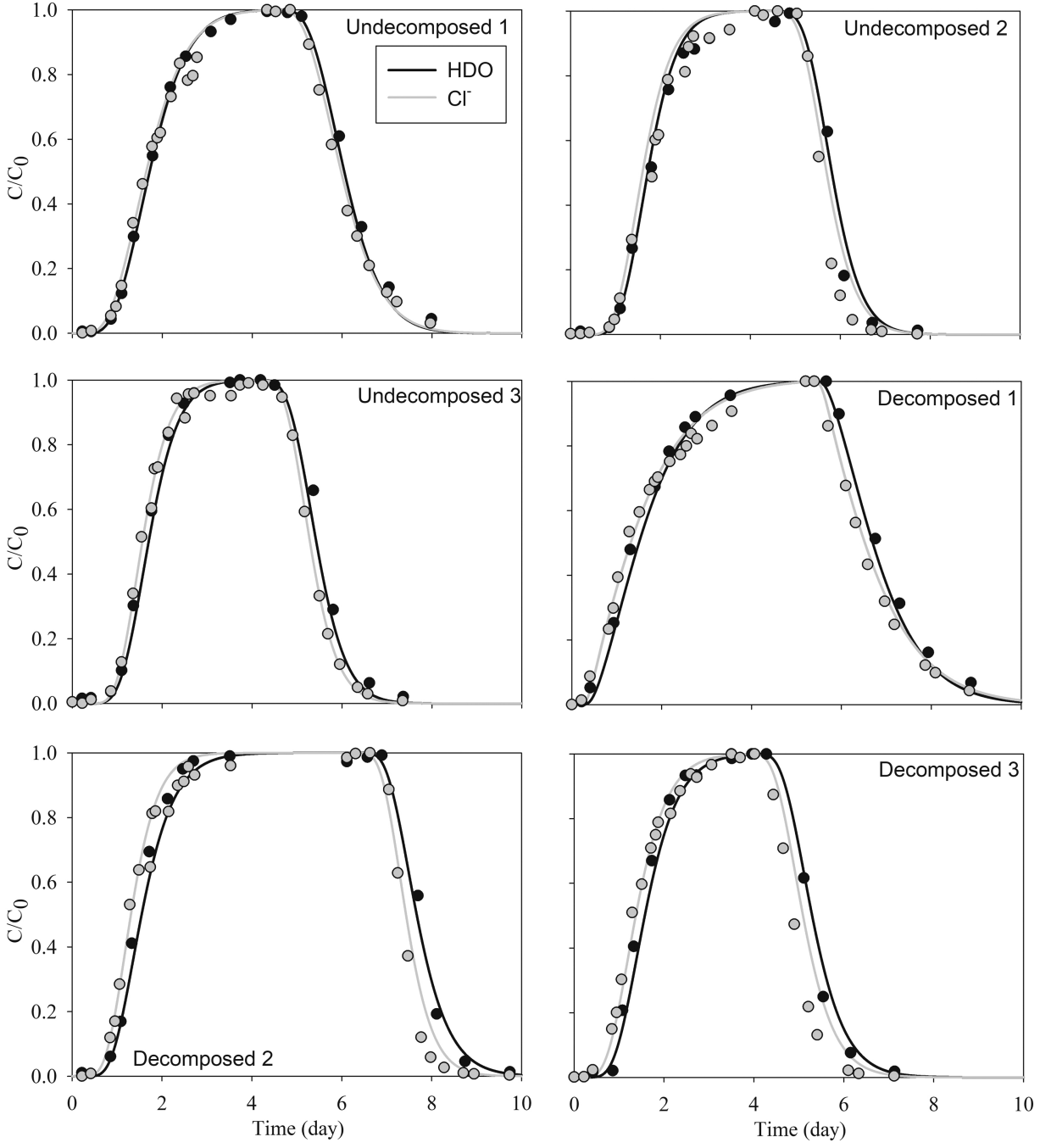
Undecomposed 1
HDO
Cl-
Undecomposed 2
Undecomposed 3
Decomposed 1
Decomposed 2
Decomposed 3
C/C0
Time (day)
0.0
0.2
0.4
0.6
0.8
1.0
0
2
4
6
8
10

Figure 2

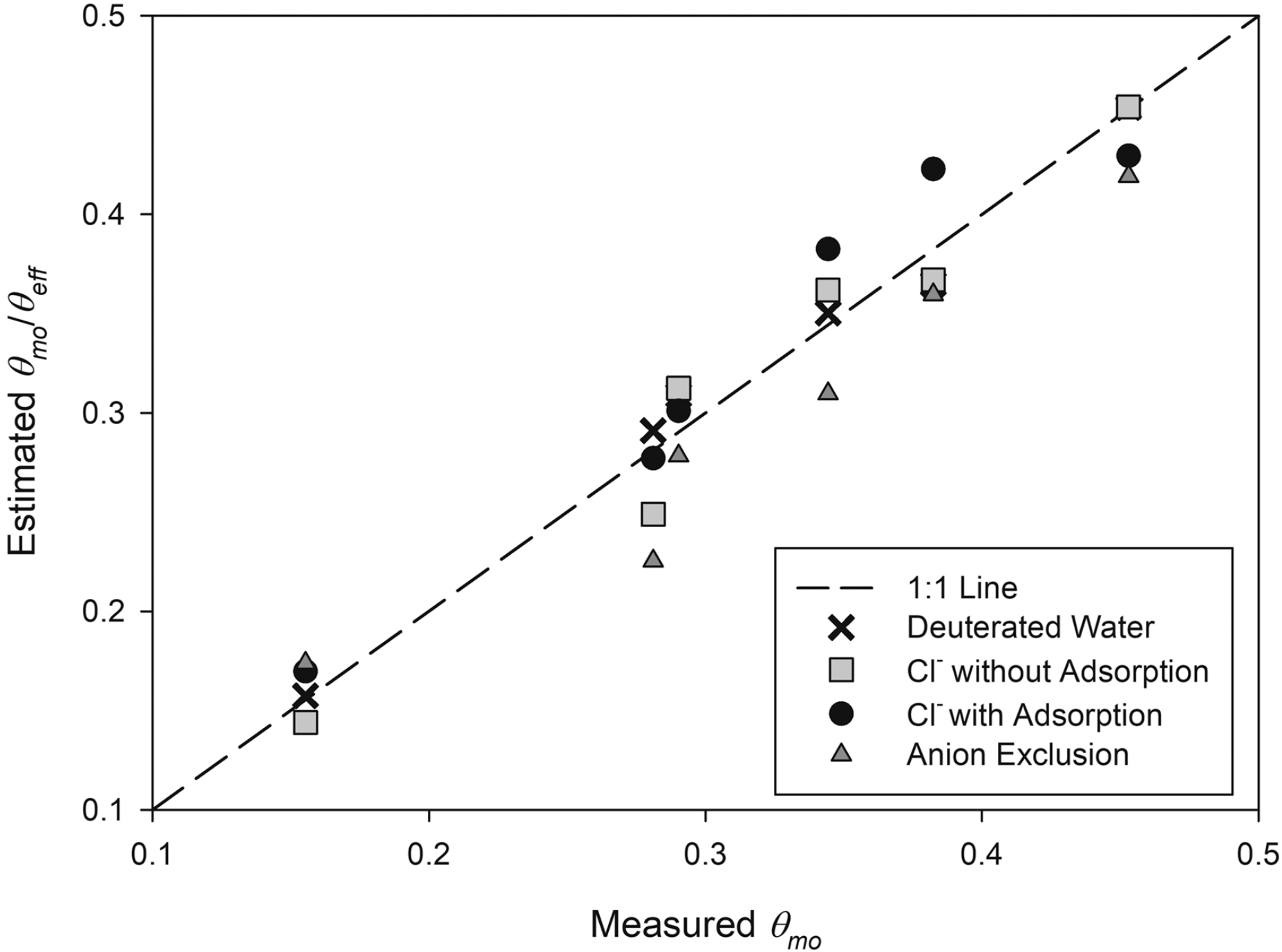
0.5
0.4
0.3
0.2
0.1
0.1
0.2
0.3
0.4
0.5
Estimated θ_{mo}/θ_{eff}
Measured θ_{mo}
1:1 Line
Deuterated Water
Cl⁻ without Adsorption
Cl⁻ with Adsorption
Anion Exclusion

Figure 3

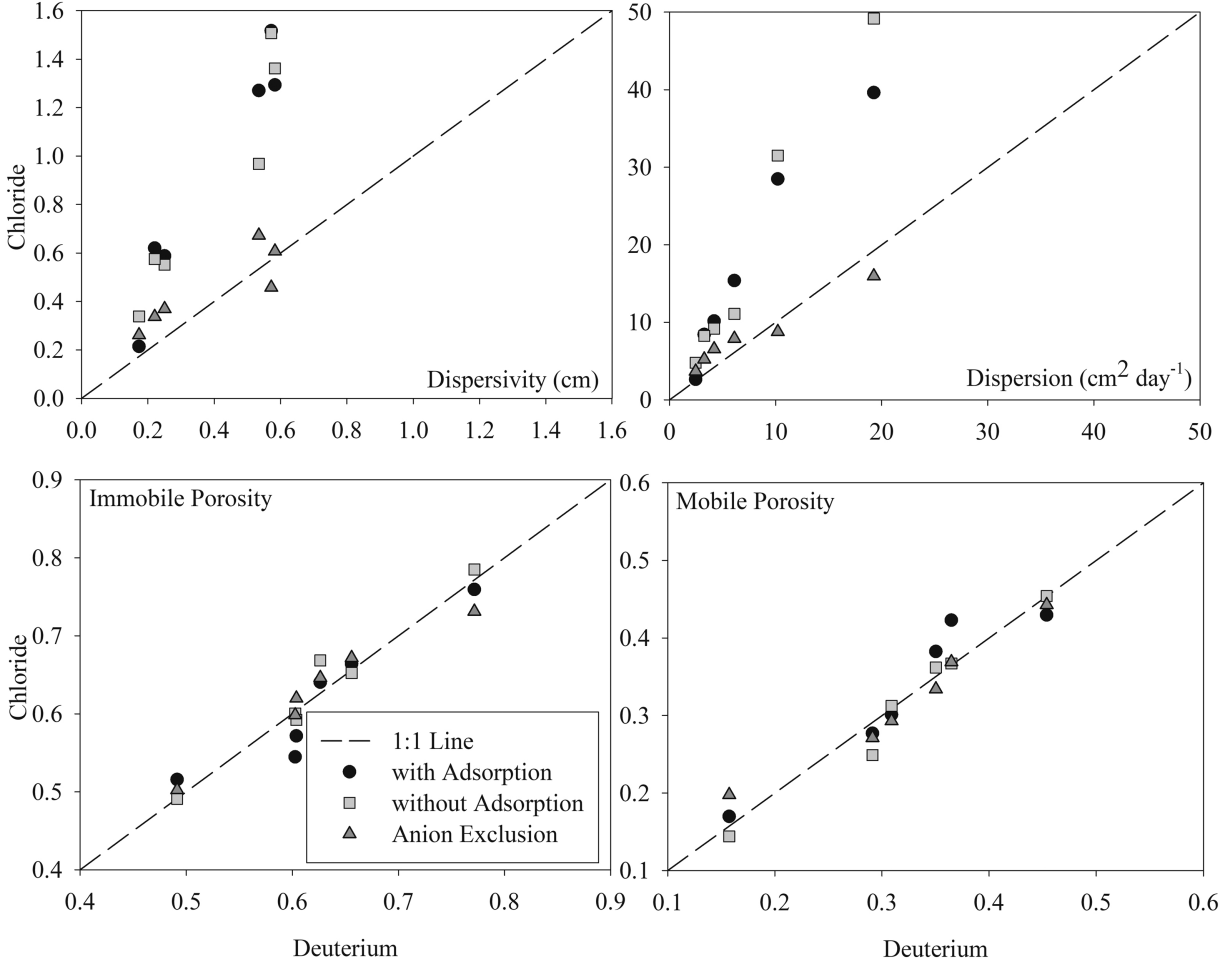
Chloride
Dispersivity (cm)
Dispersion (cm2 day-1)
Immobile Porosity
Mobile Porosity
Deuterium
Deuterium
1:1 Line
with Adsorption
without Adsorption
Anion Exclusion

Figure 4

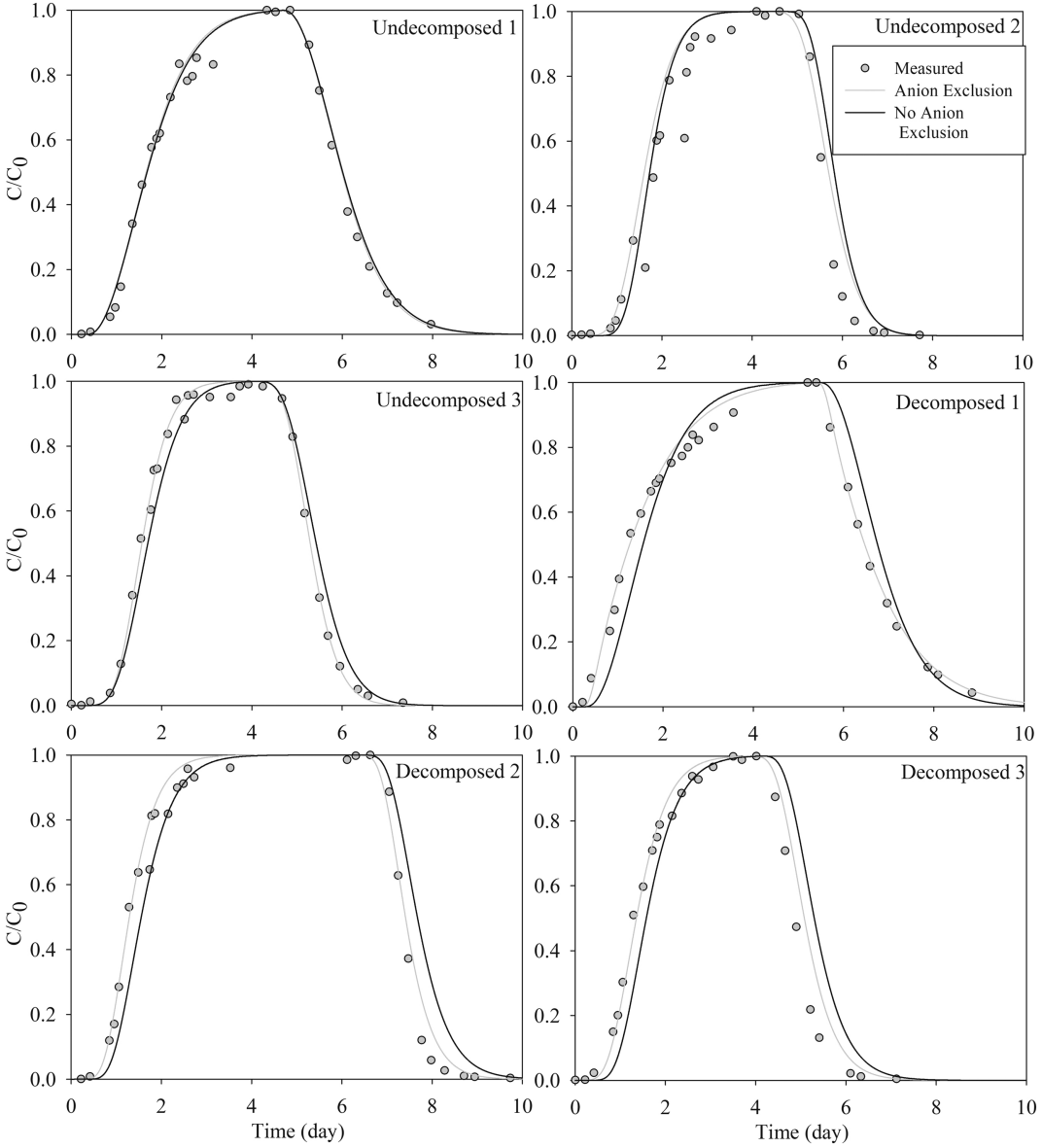
Undecomposed 1
Undecomposed 2
Undecomposed 3
Decomposed 1
Decomposed 2
Decomposed 3
Measured
Anion Exclusion
No Anion Exclusion
C/C0
Time (day)

Figure 5